MOLECULAR AND CELLULAR BIOLOGY, Feb. 2006, p. 1272–1287 Vol. 26, No. 4
0270-7306/06/$08.00+0 doi:10.1128/MCB.26.4.1272–1287.2006

hUPF2 Silencing Identifies Physiologic Substrates of Mammalian Nonsense-Mediated mRNA Decay†

Jürgen Wittmann,[1] Elly M. Hol,[2] and Hans-Martin Jäck[1]*

Division of Molecular Immunology, Department of Internal Medicine III, Nikolaus Fiebiger Center, University of Erlangen-Nürnberg, D-91054 Erlangen, Germany,[1] and Netherlands Institute for Neuroscience, Research Team Cellular Quality Control, Meibergdreef 33, 1105 AZ Amsterdam, The Netherlands[2]

Received 21 December 2004/Returned for modification 22 January 2005/Accepted 28 November 2005

Nonsense-mediated mRNA decay (NMD) is a conserved eukaryotic surveillance pathway that selectively degrades aberrant mRNAs with premature termination codons (PTCs). Although a small number of cases exist in mammals, where NMD controls levels of physiologic PTC transcripts, it is still unclear whether the engagement of NMD in posttranscriptional control of gene expression is a more prevalent phenomenon. To identify physiologic NMD substrates and to study how NMD silencing affects the overall dynamics of a cell, we stably down-regulated hUPF2, the *h*uman homolog of the yeast NMD factor *UPF2*, by RNA interference. As expected, hUPF2-silenced HeLa cells were impaired in their ability to recognize ectopically expressed aberrant PTC transcripts. Surprisingly, hUPF2 silencing did not affect cell growth and viability but clearly diminished phosphorylation of hUPF1, suggesting a role of hUPF2 in modulating NMD activity through phosphorylation of hUPF1. Genome-wide DNA microarray expression profiling identified 37 novel up-regulated and 57 down-regulated transcripts in hUPF2-silenced cells. About 60% of the up-regulated mRNAs carry typical NMD motifs. Hence, NMD is important not only for maintaining the transcriptome integrity by removing nonfunctional and aberrant PTC-bearing transcripts but also for posttranscriptional control of selected physiologic transcripts with NMD features.

Eukaryotes have acquired numerous ways to control the integrity and quality of transcripts; one of them is the so-called nonsense-mediated mRNA decay (NMD). This posttranscriptional mRNA surveillance pathway recognizes and degrades aberrant (nonsense) transcripts with premature termination codons (PTCs), thereby preventing accumulation of truncated nonfunctional or potentially noxious polypeptides as well as dissipation of energy for translating aberrant mRNA. The physiological relevance of NMD is demonstrated in several pathological situations, where NMD-resistant nonsense mRNAs accumulate. For example, the presence of stable nonsense mRNAs encoding truncated β-globin or β-amyloid precursor protein correlates with the onset of β^0-thalassemia (52) or the formation of neuritic plaques in Alzheimer's patients (65), respectively.

NMD was first observed in *Saccharomyces cerevisiae* (40) and *Caenorhabditis elegans* (23) and seems to operate in all eukaryotes, including mammals (13). Recently, homologs of the three yeast NMD factors Upf1p, Upf2p, and Upf3p (for *Up f*rameshift *p*rotein) have been identified in humans. hUPF1/rent1 (3, 41, 45, 56, 58), the *h*uman homolog of yeast *UPF1*/*re*gulator of *n*onsense *t*ranscripts, is an ATP-dependent RNA helicase (5), can be phosphorylated at serine residues in SQ motifs (55, 70), and resides in the cytoplasm (3), although it can enter the nucleus (46). hUPF1 is supposed to trigger efficient degradation of nonsense transcripts once it has been recruited to the mRNA by hUPF2/rent2. hUPF2 can also be phosphorylated (12), has no known enzymatic activity, shows strong perinuclear staining, and interacts not only with hUPF1 (41) but also with hUPF3, a nucleocytoplasmic shuttle protein and component of the exon junction complex (29, 41). Antisense RNA, RNA interference (RNAi), and dominant-negative approaches identified hUPF1 and hUPF2 as critical NMD factors involved in reducing levels of nonsense mRNAs in human cells (46, 61, 66). NMD activity in human cells is at least in part controlled by phosphorylation and dephosphorylation of hUPF1 through the phosphoinositol-3-kinase-related kinase hSMG-1, the human homolog of the *C. elegans* NMD factor SMG-1, and a dephosphorylation complex consisting of the *C. elegans* NMD homologs hSMG-5, -6, and -7 and the phosphatase PP2A (2, 11, 14, 20, 51, 70).

Classical NMD substrates are PTC-bearing nonfunctional and aberrant transcripts that are encoded either by genes bearing inherited in-frame nonsense mutations or by unproductively rearranged immunoglobulin and T-cell receptor genes. Aberrant PTC-bearing transcripts can also originate during mRNA biogenesis through RNA polymerase mistakes as well as inaccurate or incomplete pre-mRNA splicing. In mammals, NMD usually recognizes PTC-bearing nonsense transcripts only if they can be translated, have been generated by splicing from intron-bearing pre-mRNAs, and adhere to the 55-nucleotide (nt) rule, i.e., they contain more than 55 nt downstream of the PTC an exon-exon junction that has been created by removing an intron (reviewed in reference 43). During pre-mRNA splicing, a complex of at least eight proteins is deposited ~20 nt upstream of each exon-exon junction (34, 35). This exon-exon junction complex (EJC) is displaced from the transcript during the first round of translation by ribosomes (16, 24,

* Corresponding author. Mailing address: Division of Molecular Immunology, Department of Internal Medicine III, Nikolaus Fiebiger Center, University of Erlangen-Nürnberg, Glückstraβe 6, D-91054 Erlangen, Germany. Phone: 49-9131-8535912. Fax: 49-9131-8539343. E-mail: hjaeck@molmed.uni-erlangen.de.

† Supplemental material for this article may be found at http://mcb.asm.org/.

36). If translation terminates prematurely more than 55 nt upstream of the last exon-exon junction, EJC proteins, including hUPF3 and hUPF2, will remain associated with the mRNA and recruit the NMD factor hUPF1, thereby inducing rapid mRNA degradation through 5′ or 3′ exonucleases. Since authentic translational termination codons are typically located either within the terminal exon or less than 55 nt upstream from the splice acceptor of the penultimate exon (42), 3′ ends of such transcripts are not associated with EJCs and should therefore be immune to NMD.

A small number of cases are known in mammals where NMD removes not only aberrant nonfunctional but also physiologic PTC-bearing transcripts, suggesting a more general role of NMD in regulating gene expression. Examples are mRNAs encoding certain selenoproteins (49) and alternatively spliced transcripts with PTC-bearing exons. The latter may play a pivotal part in a postulated mechanism termed RUST (*R*egulated *U*nproductive *S*plicing and *T*ranslation). RUST controls protein levels through regulated alternative splicing, which determines the ratio between NMD-resistant functional and NMD-sensitive PTC-bearing unproductive transcripts (38). Although a few examples exist for such a coupling between regulated splicing and NMD in *C. elegans* (48) and humans (32, 62, 68) and one third of human mRNA splice variants should be candidates for NMD (38), it is still unclear whether the function of NMD in posttranscriptional control of gene expression is restricted to a few substrates or is a more prevalent phenomenon.

To address this question, we impaired NMD in human HeLa cells by stably down-regulating hUPF2 through RNAi. Genome-wide expression profiling of wild-type (WT) and NMD-impaired HeLa cells in fact identified novel physiologic PTC-bearing transcripts whose levels are controlled by the NMD pathway.

MATERIALS AND METHODS

Stable knockdown of hUPF2 through RNA interference. The 19-nucleotide-long hUPF2 sequence 5′-GAAGTTGGTACGGGCACTC-3′ downstream of an AA motif and with a G+C content of approximately 58% (corresponding to nucleotide residues 1,806 to 1,824 in the human cDNA clone with the GenBank accession number AY013249) was selected and inserted as an inverted repeat into the expression vector pSUPER (see Fig. 1A) as described by Brummelkamp et al. (9). A BLAST search confirmed the absence of the selected hUPF2 sequence in other transcripts in the human GenBank database. HeLa-tTA cells (10^6) (19) were cotransfected with 12 μg of pSUPER-hUPF2 and 2.5 μg of pTRE2pur harboring a puromycin *N*-acetyltransferase gene (BD Biosciences Clontech, Heidelberg, Germany) using Superfect transfection reagent (QIAGEN, Hilden, Germany). Forty-eight hours after transfection, cells were diluted 1:10 in fresh RPMI 1640 medium (Invitrogen, Karlsruhe, Germany) supplemented with 10% fetal calf serum (Invitrogen), 100 μg/ml streptomycin, 100 U/ml penicillin, and 2 mM GlutaMAX (Invitrogen). Stable clones were selected with 0.5 μg/ml puromycin and analyzed for hUPF2 levels by Western blot analysis.

Transient knockdowns of other NMD factors through RNA interference. HeLa-tTA cells (10^6) were transfected with either hUPF1-specific short interfering RNA (siRNA) (46) obtained from MWG Biotech (Ebersberg, Germany), an hUPF2-specific siRNA (nt 1,043 to 1,063 of hUPF2 coding sequence; GenBank accession number AY013249), or lamin A/C-specific siRNA (17), the latter two obtained from Dharmacon (Lafayette, CO), using Lipofectamine 2000 according to the manufacturer's instructions (Invitrogen). For silencing of hSMG-6, HeLa-tTA cells were transfected by Amaxa nucleofection with previously described hSMG-6 short hairpin RNA (shRNA)-producing plasmids (54). Briefly, 10^6 cells were resuspended in 100 μl of Nucleofector solution R, mixed with either 5 μg of a 1:1 mix of the two hSMG-6 shRNA-encoding plasmids pSUPER-E8 and pSUPER-E10 or 5 μg empty pSUPER-puro for mock transfections. Cells were electroporated using electroporation program A-28 for HeLa cells and cultured 24 h without selection, 48 h in the presence of 1 μg/ml puromycin, and another 48 h without selection.

Antibodies. Rabbit antiactin antibodies from Sigma (Steinheim, Germany) were used at a dilution of 1:1,000, monoclonal mouse anti-BiP antibodies from BD Biosciences (Heidelberg, Germany) at a dilution of 1:250, and anti-phospho-(Ser/Thr) ATM/ATR substrate antibodies from Cell Signaling Technology (Schwalbach, Germany) at a dilution of 1:1,000. An affinity-purified rabbit antiserum directed against an hUPF1 peptide was previously described (3). An antiserum against hUPF2 was generated by immunizing rabbits (Pineda Antikörperservice, Berlin, Germany) with a bacterially produced His-tagged glutathione *S*-transferase fusion protein harboring at its C-terminal end a partial hUPF2 sequence (amino acid positions 1,066 to 1,272; accession number AAG48509). The hUPF2 antiserum was affinity purified on immobilized glutathione *S*-transferase-hUPF2$_{(1,066\ \text{to}\ 1,272)}$ and used at a dilution of 1:2,000. Antibodies against keyhole limpet hemocyanin-conjugated hUPF3a and hUPF3b peptides were prepared in rabbits, affinity purified on immobilized hUPF3a and hUPF3b peptides, and used at a dilution of 1:250. Secondary horseradish peroxidase (HRP)-conjugated goat anti-rabbit and goat anti-mouse immunoglobulin G (IgG) (heavy plus light chains) antibodies were purchased from Bio-Rad (Munich, Germany).

Western blotting and immunoprecipitation. Cells were lysed in radioimmunoprecipitation assay (RIPA) buffer (1% NP-40, 0.25% sodium deoxycholate, 0.1% sodium dodecyl sulfate [SDS], 5 mM EDTA, 50 mM Tris [pH 7.4], and protease inhibitors) on ice for 15 min, and nuclei and cell debris were removed by centrifugation. Cleared lysates were separated on 8% SDS-polyacrylamide (PAA) gels, transferred onto Protean nitrocellulose membranes (Schleicher & Schuell, Dassel, Germany), and subjected to Western blot analysis as previously described (7). Briefly, membranes were blocked with 5% nonfat dry milk (Toepfer, Dietmannsried, Germany), incubated with the appropriate unconjugated primary antibody, followed by respective secondary HRP-conjugated antibodies, and developed with the enhanced chemiluminescence (ECL) method (Amersham, Freiburg, Germany). For immunoprecipitations, lysates from 5×10^6 cells in 1 ml RIPA buffer were incubated with 5 μg of affinity-purified rabbit antibodies against hUPF1 for 3 h at 4°C; immunocomplexes were precipitated with protein G Sepharose (Amersham) overnight at 4°C, washed four times with RIPA buffer, separated on 8% SDS-PAA gels, and transferred to a membrane. Phosphorylated hUPF1 (P-hUPF1) and hUPF1 signals were visualized as described above with respective antibodies.

Construction of plasmids encoding nonsense mRNA. The Ig μ heavy chain (μHC) sense vector encoding a rearranged μHC gene was constructed by cloning a rearranged genomic VDJ segment and the complete genomic constant region of the μHC gene (Cμ1–4) into pBluescript II (Stratagene) under the control of a tetracycline regulatable promoter cassette. The μHC nonsense vector was identical to the μHC sense vector except that it contained an in-frame point mutation within exon Cμ2, which converted a BamHI site into a premature translational termination codon. β-Globin sense and nonsense vectors were described in reference 64 and kindly provided by A. Kulozik (Heidelberg, Germany). To control for transfection efficiencies, the respective WT and stop vectors were cotransfected into HeLa-tTA or H2KD cells together with a mammalian expression vector harboring a mouse cDNA for an Igκ light chain (κLC) under the control of a cytomegalovirus enhancer/promoter.

Northern blot analysis. Total RNA from HeLa-tTA or H2KD cells was prepared with the RNeasy mini kit (QIAGEN) and analyzed by Northern blotting as described previously (25). Briefly, RNA was separated on 1.2% denaturing agarose-formaldehyde gels and transferred onto GeneScreen Plus membrane (PerkinElmer, Zaventems, Belgium). Hybridizations with radioactively labeled DNA probes and subsequent washings were performed as previously described (25). Radioactive bands were detected by autoradiography and with a Fujifilm FLA 3000 phosphorimager. Imaging plates were analyzed using the BASReader software program and quantified with the AIDA image analyzer (Raytest, Straubenhardt, Germany).

RT-PCR analyses. Total RNA was extracted from HeLa-tTA and H2KD cells with the RNeasy mini kit from QIAGEN and treated with DNase I (QIAGEN). First-strand cDNA was synthesized from 3 μg oligo(dT)-primed RNA with the Superscript II kit from Invitrogen. cDNAs were amplified with BioTherm *Taq* polymerase (GeneCraft, Lüdinghausen, Germany) and specific single-stranded DNA primers for 28 PCR cycles (denaturation, 94°C for 30 s; annealing, 50°C for 25 s; extension, 72°C for 100 s for TfR2 and hUPF2 and 45 s for other cDNAs). PCR products were separated on agarose gels, visualized by ethidium bromide staining, gel purified, and in the case of TfR2, cloned into Invitrogen's TA cloning vector. For quantitative real-time reverse transcriptase (RT) PCR (qRT-PCR) analysis, cDNA reaction mixtures were mixed with 2× ABsolute qRT-

TABLE 1. PCR primers used in this study

Analysis and primer	Forward sequence (5′ to 3′)	Reverse sequence (5′ to 3′)	Amplicon (bp)
RT-PCR			
TfR2	AGCTGGTGTACGCCCACTAC	CACGTACTGGGAAAGGAAGTAGA	Several
TfR2 E15-16	ACAGCAGTGCCTATTCCTTCAC	CCCAGAGAACTCGTTGAGGTT	284/369
PTGS2	TCCTGGCGCTCAGCCATACA	GTAGCCATAGTCAGCATTGTA	335
DSP	CAATGGTGTTACAGATGGCTAC	GTGAAGTCTGAGAGTGGATCTG	263
PYGM	TCAAGAGGGAGCCCAATAAGT	TGGTCAAGCTTATCCACATCC	400
FLJ22655	TCTCCCTCACAAGTGAGCTTC	CATCATTTCCACCTCCAGAGA	290
CACNB2	AGAACATTGCAGTTGGTGGTC	GTACGGCTAAGGAGAGGGTTG	341
BAG1	AAATGGAAACACCGTTGTCAG	CCAAGCCTTTCCTTTTCAATC	339
hUPF2	TGCGAGATACGTCACAATGGT	TTGCAGCAAGTTGAGAGGACA	1,367
β-actin	CAAGAGATGGCCACGGCTGCT	TCCTTCTGCATCCTGTCGGCA	275
qRT-PCR			
PTGS2	GGCTTCCATTGACCAGAGCAG	GCCGAGGCTTTTCTACCAGA	194
DSP	GCAGGATGTACTATTCTCGGC	CCTGGATGGTGTTCTGGTTCT	105
PYGM	CTGCATTTCACACTCGTAAAGGA	GCGTCCGTCCCATATAGAACT	181
FLJ22655	ACAGTGAGGTTTCTTACTAAGCG	TCTGTGTTTGAGAACAAGGGTC	133
CACNB2	CGAGTACGGGTGTCCTATGGT	TAGCTGACATTTGTCCGAACC	179
BAG1	TGCCGGGTCATGTTAATTGGG	AGAACCAGTGTGAGAGTAGGAAA	287
hUPF2	GTTGGTACGGGCACTCTTCAT	CCCCCTCAGCATGGAACAAA	130
β-actin	CTACGAGCTGCCTGACGG	GCCACAGGACTCCATGCCC	103
hSMG-5	TCCACACTAAGCGGCTTTACC	TTCCTCAGGCTAATGTTTTCTGG	118
hSMG-6	TGGGACCTCGGCTTTTGTTT	CGTCTGAGTCTTTAGAGCAGGTT	125

PCR SYBR green ROX mix (Abgene, Hamburg, Germany) and the appropriate primers and filled with water to 20 μl. qRT-PCRs were performed in triplicates in an Applied Biosystems 7300 real-time PCR system (Applied Biosystems Darmstadt, Germany) with 15 min as initial stage at 95°C to activate the DNA polymerase, followed by 40 PCR cycles of 95°C for 15 s and 60°C for 1 min. Dissociation curves were generated by heating to 95°C for 15 s, 60°C for 30 s, and 95°C for 15 s. Standardization was performed by quantification of the β-actin gene as an endogenous control. Statistical analysis was performed on at least three independent experiments. Primers (from Invitrogen) used for conventional and qRT-PCR are listed in Table 1.

Analysis of cell growth and viability. To analyze cell growth, 1×10^5 cells in 2 ml RPMI 1640 medium were seeded in six-well plates in triplicate and cultured for 3 days. Every 24 h, cells were trypsinized, stained with trypan blue, and counted using a hemocytometer. For analyses of cellular DNA content, up to 4×10^5 cells were suspended in 400 μl of a hypotonic 0.1% sodium-citrate solution, 50 μg/ml propidium iodide (PI; Merck, Darmstadt, Germany), and 0.1% Triton X-100 and incubated at 4°C for at least 1 h. PI fluorescence was analyzed by flow cytometry (EPICS XL3; Beckman Coulter, Krefeld, Germany), and frequencies of cells in the individual cell cycle phases were calculated with the ModFit LT software (BD Biosciences). Frequencies of dead cells were calculated from signals in the sub-G_1 phase.

Oligonucleotide microarray analysis. Total RNA was isolated from mid-confluent-phase WT and H2KD cells with Trizol reagent (Invitrogen) and further purified using an RNeasy mini kit (QIAGEN). Residual traces of genomic DNA were removed with DNase I (QIAGEN). For first-strand cDNA synthesis, 13.5 μg of total RNA was annealed with a mixture of three polyadenylated control RNAs and 100 μM of a T7-oligo$(dT)_{24}$-V primer [5′-GCATTAGCGGCCGCG AAATTAATACGACTCACTATAGGGAGA-$(dT)_{24}$V-3′; MWG Biotech] for 10 min at 70°C. The first strand was synthesized at 42°C for 1 h with 200 U of Superscript II (Invitrogen); the second strand was completed first with 40 U *Escherichia coli* DNA polymerase I (Invitrogen), 12 U *E. coli* DNA ligase (TaKaRa; BioWhittaker, Taufkirchen, Germany), and 2 U RNase H (TaKaRa) at 16°C for 2 h and then with 10 U T4 DNA polymerase I (TaKaRa) for 5 min at 16°C. The reaction was stopped with 10 μl 0.5 M EDTA; cDNA was extracted with phenol-chloroform, and the aqueous phase was recovered by Phase Lock Gel separation (Eppendorf, Hamburg, Germany). Precipitated cDNA was dissolved in RNase-free water and used to synthesize biotinylated cRNA using the BioArray high yield RNA transcript labeling kit from Enzo Diagnostics (Santa Clara, CA). Labeled cRNA was purified using the RNeasy mini kit (QIAGEN). Fragmentation of cRNA, hybridization to HG-U133A microarrays (Affymetrix, High Wycombe, United Kingdom), washing, and staining as well as scanning of the arrays in a GeneArray scanner (Agilent, Böblingen, Germany) were performed as recommended in the Affymetrix gene expression analysis technical manual. Signal intensities and detection calls were determined using the GeneChip 5.0 software. A scaling across all probe sets of a given array to an average intensity of 1,000 units was included to compensate for variations in the amount and quality of the cRNA samples and other experimental variables. To detect differentially expressed genes, comparison files were further filtered using the Affymetrix Data Mining Tool 3.0 software. Filter criteria included a change of "I," a signal log ratio of >1, and a detection *P* value of <0.001 or a change of "D," a signal log ratio of <−1, and a detection *P* value of >0.999.

Bioinformatics. To compare RNA to genomic sequences, we used either the Spidey mRNA-to-genomic alignment program (http://www.ncbi.nlm.nih.gov/IEB/Research/Ostell/Spidey/spideyweb.cgi) or the UCSC genome browser (http://genome.ucsc.edu/cgi-bin/hgGateway). Public sequence databases as well as Celera's annotated human genome were browsed with gene symbol entries using Celera's interactive graphical viewer, myScience Map Viewer (http://myscience.appliedbiosystems.com/). Information about a protein's molecular functions was retrieved from Celera's Panther (http://myscience.appliedbiosystems.com), Weizmann's GeneCards (http://bioinfo.weizmann.ac.il/cards/index.shtml), and Swissprot/TrEMBL (http://au.expasy.org/cgi-bin/sprot-search-ful) databases. The database for alternative splice forms with NMD features was described previously (38) and can be accessed at http://compbio.berkeley.edu/people/ed/rust/Results.html.

RESULTS

To identify physiologic NMD substrates and to realize the significance of NMD in the general regulation of gene expression, we impaired NMD in human cells by transiently as well as stably down-regulating hUPF2 through RNAi using chemically produced siRNA and plasmids encoding shRNA (17), respectively. We decided to stably express hUPF2-specific siRNA-like transcripts from a polymerase III expression vector in the human HeLa cell line, which should result in the continuous delivery of hUPF2 shRNA transcripts and a lasting suppression of NMD. This approach will allow not only the identification of novel physiologic NMD substrates by genome-wide expression profiling techniques but also the analysis of NMD-silencing phenotypes in long-term cultured cells.

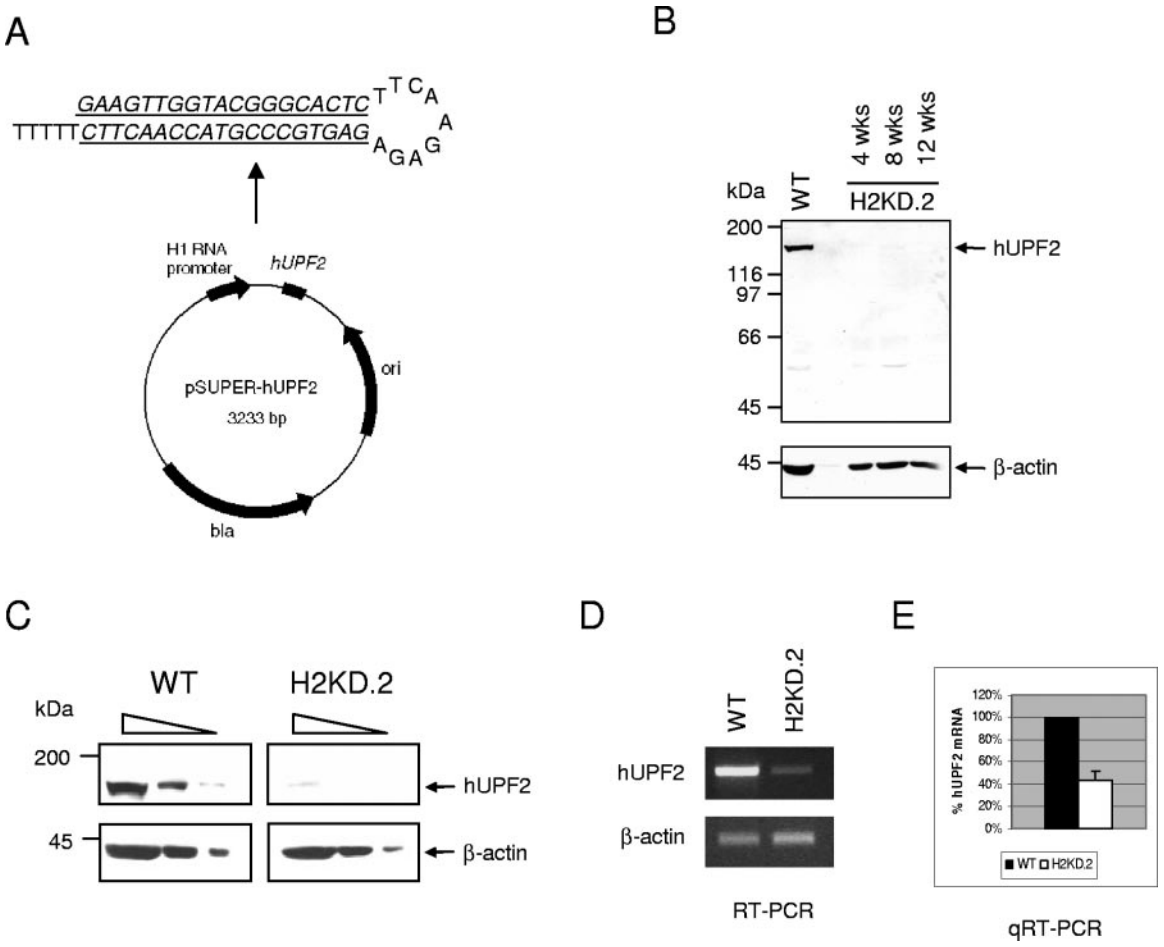

FIG. 1. Stable silencing of hUPF2 in HeLa cells. (A) Schematic presentation of the pSUPER-hUPF2 vector. A DNA fragment consisting of the 19-nt hUPF2 sequence followed by a 9-nt spacer and the 19-nt reverse hUPF2 sequence was cloned downstream of the H1 RNA promoter. The predicted structure of the hUPF2 shRNA is shown above with the 19-nt hUPF2 sequence underlined. (B) Western blot analysis of hUPF2 in HeLa (WT) cells and a clone stably transfected with an hUPF2 shRNA-encoding plasmid (H2KD.2). Cellular proteins were reduced, separated by 8% SDS-PAGE, and transferred to a nitrocellulose membrane, which was first stained with polyclonal rabbit anti-hUPF2 antibodies (hUPF2) and developed with an appropriate HRP-conjugated secondary antibody and the ECL method. Loading of equal cell equivalents was assessed with rabbit antibodies against β-actin. Molecular masses of standard proteins are indicated in kDa on the left. (C) Western blot analysis of hUPF2 in serially diluted cell lysates from HeLa (WT) and H2KD.2 cells. Analysis was performed as described in panel B with polyclonal rabbit antibodies against hUPF2 and β-actin. The lanes represent threefold serial dilutions of protein. (D) RT-PCR analysis of hUPF2 mRNA in WT and H2KD.2 cells. PCR products were separated on a 1.5% agarose gel and stained with ethidium bromide. Loading of same cell equivalents was assessed by analyzing β-actin mRNA levels (lower panel). Results represent one of two independent experiments. (E) Analysis of hUPF2 mRNA in WT and H2KD.2 cells by qRT-PCR. Relative hUPF2 mRNA levels were determined and normalized to β-actin mRNA levels, which served as an internal control. The amount of hUPF2 mRNA in WT cells was set to 100%. Average values and standard deviations of three independent qRT-PCR runs (triplicates for each) are shown.

Establishment of HeLa clones with a stable knockdown (KD) of hUPF2 by RNAi. We first designed a double-stranded DNA (dsDNA) oligonucleotide that is flanked by appropriate restriction overhangs and consists of a 19-nt sequence derived from hUPF2, followed by a short spacer and the reverse complement of the 19 nt. The dsDNA fragment was inserted downstream of the H1 RNA polymerase III promoter into the expression plasmid pSUPER (Fig. 1A) (9). The inserted hUPF2 sequence encodes a transcript that should form an hUPF2-specific shRNA (at the top of Fig. 1A), which can be targeted to the RNAi machinery like an siRNA molecule. pSUPER-hUPF2 was cotransfected with a plasmid harboring a puromycin *N*-acetyltransferase gene into human HeLa cells. Stable puromycin-resistant HeLa clones were selected and analyzed for hUPF2 levels by Western blot analysis (Fig. 1B). While specific rabbit antibodies clearly detected hUPF2 with the expected molecular mass of 147 kDa in untransfected HeLa cells (designated as "WT" throughout the rest of this paper), hUPF2 protein was virtually absent in the puromycin-resistant *h*UPF*2* *k*nock-*d*own clone 2 (H2KD.2), even after these cells were continuously cultured for up to 12 weeks and longer (Fig. 1B). The same results were obtained with the H2KD.3 clone (data not shown). To quantify the degree of hUPF2 silencing at the protein level, we performed Western blot analysis of threefold serially diluted lysates from equal numbers of WT and hUPF2-silenced H2KD cells. As shown in Fig. 1C (upper row), an hUPF2 signal could still be detected in a 1:9 diluted lysate from the WT but was barely visible in an

undiluted lysate in H2KD.2 cells, suggesting that the hUPF2 protein level was reduced in H2KD cells to 10% of that in WT cells or even less. shRNA-mediated down-regulation of hUPF2 expression in H2KD cells was verified at the mRNA level by conventional RT-PCR (Fig. 1D) and quantified by DNA microarray analyses and qRT-PCR (Fig. 1E). Surprisingly, both microarray (see Table S1 in the supplemental material) as well as qRT-PCR analysis revealed that hUPF2 was decreased at the mRNA level by approximately 60% (Fig. 1E), which is clearly above the 90% reduction of hUPF2 at the protein level in H2KD cells. Hence, hUPF2-specific shRNA not only induces mRNA degradation but in analogy to microRNA (15), might also affect translation.

hUPF2 controls steady-state levels of ectopically expressed nonsense transcripts. The effect of stable hUPF2 silencing on a cell's ability to reduce levels of nonsense mRNAs was assessed by transiently transfecting WT and H2KD cells with plasmids encoding either a functional transcript or its corresponding nonsense counterpart with an in-frame PTC. We chose nonsense transcripts encoding mouse μHC (26) and human β-globin mRNAs (64) as well-characterized NMD model substrates. Cotransfection of a plasmid carrying a rearranged mouse κLC gene controlled for differences in transfection efficiencies. Total RNA was isolated 48 h after transfection of WT and H2KD.2 cells with sense and nonsense expression constructs, and Northern blotting was performed with specific radiolabeled DNA probes. Signal intensities were quantified by phosphorimaging, and relative steady-state levels of WT and nonsense transcripts were calculated by dividing their experimental signals by κLC signals. Relative mRNA levels of sense transcripts in WT cells were arbitrarily set to 100%.

As expected, relative levels of sense transcripts encoding either β-globin (Fig. 2A) or μHC (Fig. 2B) did not significantly change in hUPF2-silenced H2KD cells compared to those of WT cells. In contrast, relative nonsense β-globin (Fig. 2A) as well as nonsense μHC (Fig. 2B) mRNA levels showed an approximately threefold increase in hUPF2-silenced H2KD.2 cells. Nonsense transcripts in H2KD.2 cells, however, did not reach the level of the corresponding sense transcripts but accumulated to 65% and 40% of that observed for β-globin and μHC sense transcripts, respectively. Similar results were obtained when we transiently cotransfected HeLa cells with a synthetic hUPF2-specific siRNA and the nonsense β-globin or the nonsense μHC reporter gene (data not shown). Hence, stable hUPF2 silencing results in a lasting impairment of NMD, which confirms findings obtained for HeLa cells by transiently reducing hUPF2 levels with siRNA (46) or antisense transcripts (66).

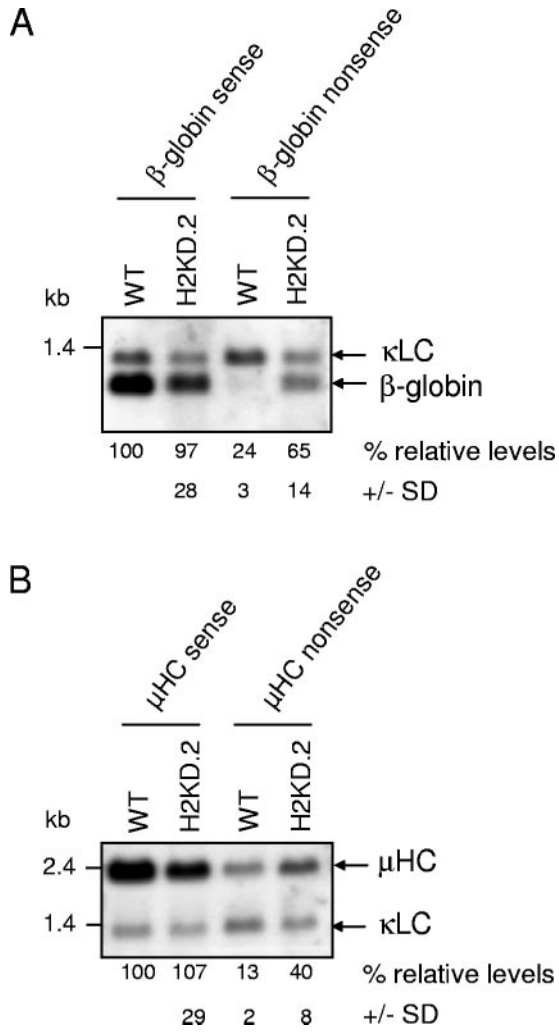

FIG. 2. Analysis of ectopic nonsense mRNA levels in hUPF2-silenced cells. WT and H2KD.2 cells were transfected with plasmids encoding either sense or PTC-containing nonsense β-globin (A) or μHC transcripts (B) and, in order to control for transfection efficiency, with a plasmid encoding κLC. Total RNA was isolated 48 h after transfection, separated on a 1.2% agarose-formaldehyde gel, and subjected to Northern blot analysis. Fifty percent more RNA from cells transfected with nonsense vectors was loaded. Radioactive signals were quantified by phosphorimaging. Relative transcript levels were calculated by dividing β-globin and μHC signals by corresponding κLC signals; relative intensities of sense transcripts in WT cells were arbitrarily set to 100%. Mean values and standard deviations (SD) were calculated from three independent experiments.

Silencing of hUPF2 affects phosphorylation of hUPF1 but not expression of other NMD factors. NMD activity in human cells is controlled by phosphorylation and dephosphorylation of hUPF1 (2, 11, 14, 20, 51, 70). Genetic studies of *C. elegans* revealed that phosphorylation of SMG-2, the *C. elegans* ortholog of hUPF1, requires the presence of SMG-3 and SMG-4, the *C. elegans* orthologs of hUPF2 and hUPF3, respectively (53). Whether mammalian hUPF2 also plays a role in phosphorylation of hUPF1 is not known and could be addressed in our stable hUPF2-silenced HeLa clones, but only if silencing of hUPF2 did not affect the overall levels of hUPF1 and hUPF3. Indeed, Western blot analyses of threefold serially diluted lysates from equal cell numbers revealed almost identical steady-state levels of hUPF1 as well as hUPF3a and hUPF3b in WT and hUPF2-silenced H2KD cells (Fig. 3). In addition, qRT-PCR analysis revealed in WT and stably hUPF2-silenced H2KD cells almost identical levels of hSMG-5 and hSMG-6 mRNA (data not shown), two other NMD factors known to play a role in hUPF1 dephosphorylation (11). These findings are in agreement with results from our genome-wide DNA microarray analyses, which did not reveal significant up- or down-regulation of hUPF1, hUPF3a, hUPF3b, hSMG-5, and hSMG-6 mRNA levels in hUPF2-silenced H2KD cells (data not shown).

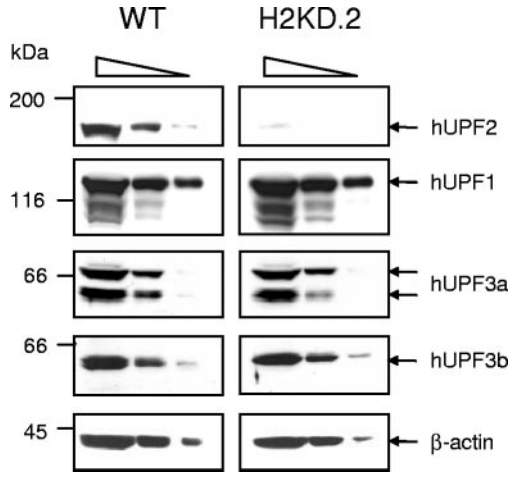

FIG. 3. Analysis of hUPF protein levels in hUPF2-silenced cells. Cellular lysates from 4.5×10^5, 1.5×10^5, and 0.5×10^5 WT or H2KD.2 cells were reduced, separated by 8% SDS-PAGE, and transferred to a nitrocellulose membrane. The membrane was stained stepwise with anti-hUPF2, anti-hUPF1, anti-hUPF3a, and anti-hUPF3b antibodies and developed with an appropriate HRP-conjugated secondary antibody and the ECL method. Loading of same cell equivalents was assessed with rabbit antibodies against β-actin. Results correspond to one of two independent experiments. The lanes represent threefold serial dilutions of protein and demonstrate that the Western blotting is semiquantitative. Molecular masses of standard proteins are indicated in kDa on the left. The Western blots for hUPF2 and β-actin are identical to the ones shown in Fig. 1C and have been included in Fig. 3 for clarity.

If hUPF2 is involved in controlling the phosphorylation of hUPF1, we would expect a change in levels of phosphorylated hUPF1 in hUPF2-silenced H2KD cells. To address this question, we first precipitated hUPF1 from lysates of equal numbers of WT and hUPF2-silenced H2KD cells with a specific rabbit serum against hUPF1 (3), separated the proteins by SDS-polyacrylamide gel electrophoresis (PAGE), transferred them onto a nitrocellulose membrane, and detected phosphorylated hUPF1 with a commercially available phospho-(Ser/Thr) ATM/ATR substrate antibody. This antibody preferentially binds peptide motifs containing phosphorylated Ser or Thr preceded by Leu or a similar hydrophobic amino acid and followed by Gln. The antibody does not cross-react with corresponding nonphosphorylated sequences or with other phospho-(Ser/Thr)-containing motifs (http://www.cellsignal.com/pdf/2851.pdf). Since ATM/ATR kinases are primarily activated by DNA double-strand breaks (reviewed in reference 59) and since Leu-Ser-Gln motifs are major phosphorylation sites in the C-terminal part of hUPF1 (70), the P-(Ser/Thr) ATM/ATR substrate antibody should stain predominantly phosphorylated hUPF1 (P-hUPF1) with a molecular mass of 130 kDa. Indeed, the P-(Ser/Thr) ATM/ATR substrate-specific antibody detected in anti-hUPF1 precipitates from hUPF2-silenced H2KD cell lysates compared to WT lysates a weaker signal for the 130-kDa band, the expected molecular mass of hUPF1 (Fig. 4A, left blot). The weaker P-hUPF1 signal was not due to an overall reduction of the cellular hUPF1 level in H2KD.2 cells, since stripping and reprobing the same membrane with anti-hUPF1-specific antibodies revealed identical signal intensities of the 130-kDa hUPF1 band in anti-hUPF1 precipitates from both WT and H2KD cells (Fig. 4A, right blot). Therefore, the reduced signal of the P-(Ser/Thr) ATM/ATR substrate antibody-reactive 130-kDa band in hUPF2-silenced H2KD cells seems to be a consequence of a reduced number of phosphate residues per hUPF1 molecule rather than of lower cellular hUPF1 levels.

If the 130-kDa band detected in Fig. 4A (left blot) with the P-(Ser/Thr) ATM/ATR substrate antibody is P-hUPF1, its intensity should also decrease in hUPF1-silenced HeLa cells, or conversely, increase in cells with an impaired ability to dephosphorylate P-hUPF1. In accordance with our first prediction, decreased signals of the 130-kDa band were detected by Western blotting with the P-(Ser/Thr) ATM/ATR substrate antibody in twofold serially diluted cellular lysates from transiently hUPF1 siRNA-transfected HeLa cells (Fig. 4B, first blot) and, after stripping the same membrane, with specific anti-hUPF1 antibodies (Fig. 4B, second blot). The decrease in hUPF1 signals in HeLa cells transfected with hUPF1 siRNA is not the consequence of differences in loaded protein amounts, as signals for hUPF2 and β-actin were almost identical (Fig. 4B, blots 3 and 4, respectively). In addition, the reduction of hUPF1 signals is specific for hUPF1 siRNA, as hUPF1 levels did not change in HeLa cells transiently transfected with lamin A/C siRNA compared to those with mock transfections.

Conversely, down-regulation of hSMG-6, the human homolog of *C. elegans* SMG-6 (11, 18) and a cofactor involved in dephosphorylation of hUPF1 (11), reduced hSMG-6 levels by approximately 60% (see Fig. S1 in the supplemental material) by transiently transfecting HeLa cells with a plasmid encoding an hSMG-6-specific shRNA (54) and resulted in a stronger signal of the anti-P-(Ser/Thr) ATM/ATR substrate antibody-reactive 130-kDa band (Fig. 4C, first blot). The increase of the 130-kDa band was specific, as levels of hUPF2 and the chaperone BiP did not change in hSMG-6 shRNA-transfected HeLa cells compared to levels in mock-transfected cells (Fig. 4C, blots 2 and 3, respectively). These findings not only complement a previous report by Chiu and coworkers, who showed that overexpression of hSMG-6 leads to a decrease in hUPF1 phosphorylation (11), but also identify the P-(Ser/Thr) ATM/ATR substrate antibody-reactive 130-kDa band as hUPF1.

In summary, we have identified by three independent approaches (Fig. 4A to C) the anti-P-(Ser/Thr) ATM/ATR substrate antibody-reactive 130-kDa band as phosphorylated hUPF1; thus, hUPF2 directly or indirectly controls the phosphorylation of hUPF1 in mammalian cells. However, reduction of hUPF1 phosphorylation in response to an hUPF2 knockdown is not the result of increased mRNA levels of the hUPF1-dephosphorylating NMD factors hSMG-5 and hSMG-6 (11), since levels of both transcripts did not change in hUPF2-silenced HeLa (H2KD) cells, as revealed by qRT-PCR.

Effect of hUPF2 silencing on growth and survival of human HeLa cells. The human cervix cancer line HeLa can be cultured for a long period despite an impaired NMD and barely detectable levels of hUPF2. This is in line with the finding that NMD is not essential for viability of yeast cells, since deletion of any of the three yeast *UPF* genes leads to only a minimal impairment in respiration (1) and an increased sensitivity to chemical inhibitors of translation (33). Nevertheless, it is still possible that hUPF2-silenced cells survive but have a growth disadvantage compared to WT HeLa cells. This, however, seems not to be the case, since the increase in numbers over

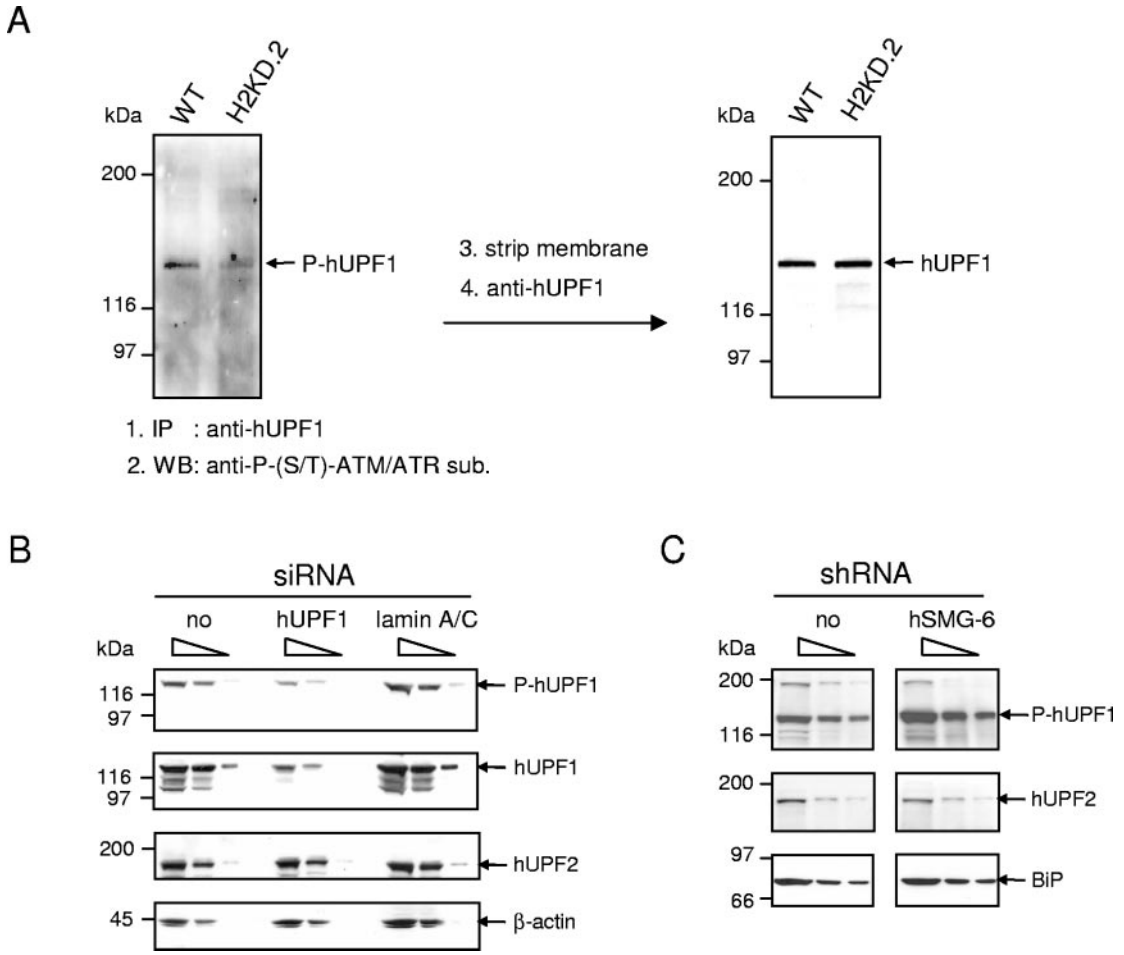

FIG. 4. Analysis of hUPF1 phosphorylation in hUPF2- and hSMG-6-silenced cells. (A) Detection of P-(S/T) ATM/ATR motifs in hUPF1 by a combined immunoprecipitation (IP) and Western blot (WB) analysis. hUPF1 was precipitated from cleared lysates of 5×10^6 WT or H2KD.2 cells with specific rabbit anti-hUPF1 antibodies (IP: anti-hUPF1), electrophoretically separated, and transferred to a nitrocellulose membrane. The membrane was first developed with P-(S/T) ATM/ATR substrate-specific antibodies (WB, left blot) and, after stripping, with anti-hUPF1 antibodies (right blot). (B) Effect of hUPF1 down-regulation on the phosphorylation status of (S/T) ATM/ATR substrates. Cellular proteins from 4×10^5, 2×10^5, and 0.5×10^5 HeLa cells transfected without siRNA (no), with hUPF1 siRNA (hUPF1), and with lamin A/C siRNA (lamin A/C) were electrophoretically separated and analyzed by stepwise immunoblotting with antibodies against P-(S/T) ATM/ATR substrates (P-hUPF1), hUPF1, and hUPF2. Equal protein loading was assessed with rabbit antibodies against β-actin. The lanes represent two- and fourfold serial dilutions of protein and demonstrate that the Western blotting is semiquantitative. Molecular masses of standard proteins are indicated in kDa on the left. (C) Effect of hSMG-6 down-regulation on the phosphorylation status of hUPF1. Cellular proteins from 2×10^5, 1×10^5, and 0.5×10^5 HeLa cells transiently transfected with the empty pSUPER-puro vector (no) or pSUPER-puro encoding hSMG-6-specific shRNAs (hSMG-6) were electrophoretically separated and analyzed by stepwise immunoblotting with antibodies against P-(S/T) ATM/ATR substrates (P-hUPF1) and hUPF2. BiP stainings served as a control for protein loading. The lanes represent twofold serial dilutions of total lysates. Cellular lysates in panels A, B, and C were reduced and separated on 8% SDS-PAA gels, and signals were developed with appropriate HRP-conjugated secondary antibodies and the ECL method. Molecular masses of standard proteins and their positions are indicated in kDa on the left, and the positions of the respective protein bands are indicated on the right of the blots. Results represent one of at least two independent experiments.

time of both WT and hUPF2-silenced H2KD cells was the same, i.e., the cells grew equally well (Fig. 5A). Further, PI stainings of nuclei revealed no significant differences in either the cell cycle distribution or the frequencies of cells in the sub-G_1 gate (representing dying cells with fragmented DNA) in WT (Fig. 5B, a) and H2KD (Fig. 5B, b) cells. Finally, compared to those of WT HeLa cells, microscopic analyses did not show any obvious morphological changes of H2KD cells (data not shown). Based on these findings, we conclude that hUPF2-silenced H2KD cells possess growth and survival properties similar to those of WT cells. To our knowledge, this is the first report of a mammalian cell line with a stable impairment of NMD.

NMD controls abundance of novel physiologic transcripts. NMD's established function is the removal of aberrant mRNA that originated either from mutated as well as unproductively rearranged genes or through incorrect or alternative processing of transcripts (reviewed in reference 43). However, as mentioned above in the introduction, there are a few reports indicating NMD in the regulation of physiologic mRNAs, i.e., transcripts that encode a functional polypeptide. To identify novel NMD substrates, we subjected both WT and hUPF2-

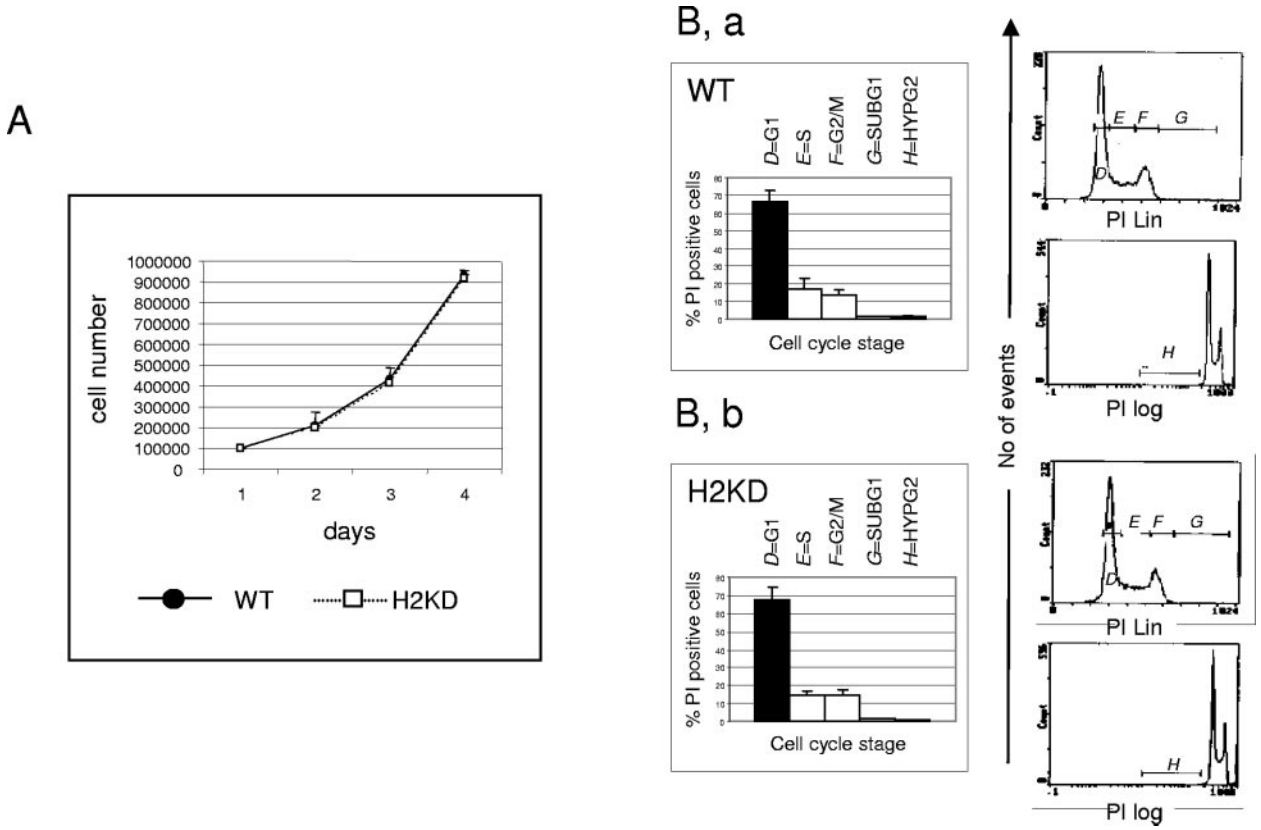

FIG. 5. Effect of hUPF2 down-regulation on cell growth and cell cycle progression. (A) Growth rates of WT (circles) and H2KD cells (boxes). Cells (1×10^5) were plated in triplicate in three six-well plates and cultured at 37°C for 3 days. Viable cells were counted every 24 h using a hemocytometer after being stained with trypan blue. Measurements were performed in triplicate in a series of three independent experiments. Standard deviations are indicated. (B) Cell cycle analysis of WT (a) and H2KD cells (b). Cells were harvested, permeabilized, and stained with PI. PI fluorescence was measured by flow cytometric analysis and analyzed with the ModFit LT software. The bar diagrams on the left illustrate the mean distributions from at least seven independent experiments of WT and H2KD cells in the sub-G_1 (gate G in the right diagram), the G_1 (gate D), the S (gate E), and the G_2/M (gate F) phases of the cell cycle; standard deviations are indicated. The diagrams on the right with either a linear (Lin) or logarithmic representation of the PI fluorescence show the distribution of WT and H2KD cells in the individual phases of the cell cycle. Gates were set to distinguish the different cell populations according to their DNA content.

silenced H2KD cells to a genome-wide expression profiling using the Affymetrix HG-U133A microarray chip. This chip contains more than 500,000 oligonucleotide DNA probes grouped in approximately 22,000 probes, which represent more than 16,000 fully annotated unique human genes. Hybridization was performed three times each with biotinylated cDNA reverse transcribed from independently isolated RNA. Only transcripts whose expression levels changed in H2KD cells by a factor of 2 in each of the three independently performed hybridization experiments with statistically significant *P* values of ≤ 0.001 or ≥ 0.999 were included in the analysis. When we applied these stringent conditions, 37 of the approximately 2,400 reproducibly detected mRNAs (1.5%) were found to be up-regulated, and 57 transcripts (2.4%) were found to be down-regulated in hUPF2-silenced H2KD compared to those in WT cells. As expected for a positive control, hUPF2 levels were decreased in analyzed H2KD samples. Complete lists of all differentially regulated genes are included in Table S1 in the supplemental material.

As shown in Fig. 6A and B, qualitative changes observed in microarray analyses could be verified for randomly selected up- and down-regulated transcripts by semiquantitative RT-PCR as well as qRT-PCR analysis. β-actin levels, which were unchanged in all microarray analyses (data not shown), controlled for equal amounts of input cDNA in both assays. The same picture was observed when we analyzed levels of selected transcripts by RT-PCR in a second stable hUPF2-silenced clone (H2KD clone no. 3) and in HeLa cells transiently transfected with a synthetic hUPF2 siRNA (data not shown). The target sequence of the synthetic hUPF2 siRNA differs from that used in stably silenced H2KD cells, thereby reducing the likelihood that the siRNA acts on other transcripts and that the observed effects are therefore indirect. The effect of hUPF2 siRNA was specific, since transiently transfected siRNA against lamin A/C did not affect levels of selected transcripts that were either down- or up-regulated in HeLa cells transiently transfected with hUPF2 siRNA (data not shown).

There are a few reports that synthetic siRNAs or shRNAs induce in a sequence-independent manner via Toll-like receptors the interferon (IFN) pathway in mammalian cells (8, 60). Usually, only double-stranded RNAs longer than 30 bp are potent inducers of type I IFN synthesis in mammalian cells (12). IFN activates among others two classes of enzymes: the dsRNA-dependent protein kinase and the 2′,5′-oligoadenylate

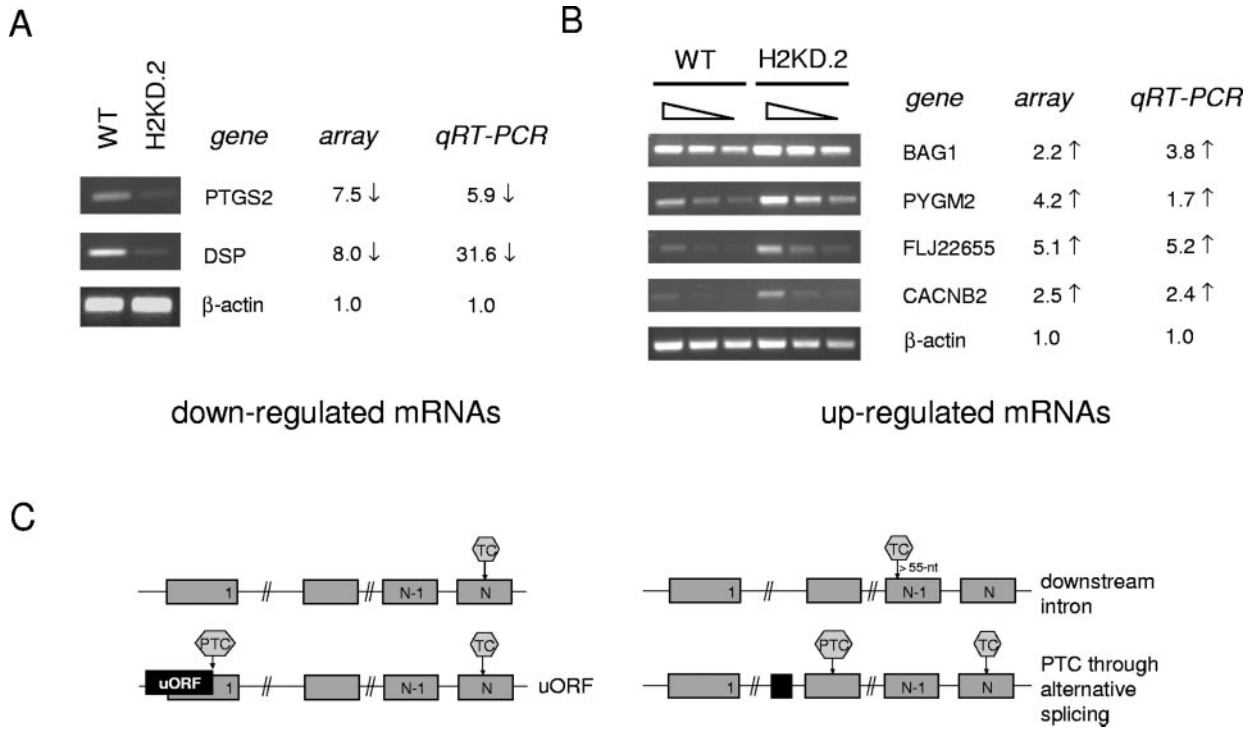

FIG. 6. Verification of DNA microarray results by semiquantitative and quantitative real-time RT-PCR analyses. Total RNA from WT and hUPF2-silenced H2KD.2 cells was analyzed by RT-PCR and qRT-PCR for the presence of selected transcripts (indicated on the right of each gel picture) that were either (A) down-regulated or (B) up-regulated in the DNA microarray analyses. RT-PCR transcripts were detected after agarose gel electrophoresis by ethidium bromide staining. β-Actin signals served to assess the loading of equal amounts of cDNA. Results represent one of two independent experiments. Differences in mRNA abundance (*n*-fold) obtained in microarray (array) and qRT-PCR analyses are indicated on the right side of the gel pictures. qRT-PCR values were normalized to β-actin mRNA levels and represent the means from at least three independent experiments, which were run in triplicate. To demonstrate a linear relationship between the amounts of input cDNA and RT-PCR products, serial dilutions of cDNA were analyzed by semiquantitative RT-PCR in panel B. (C) Schematic depiction of mRNA transcripts with possible NMD-causing features.

synthetase (OAS1), the latter of which is a potent modulator of transcript levels via activation of the nuclease RNase L. However, the differences in expression profiles between WT and H2KD cells are a consequence of hUPF2 silencing rather than of dsRNA-induced IFN signals. First, comparison of our differentially expressed genes with entries in GeneCards (Weizmann Institute) and Unigene (NCBI) databases showed that none of the up-regulated genes in hUPF2-silenced H2KD cells is a known target for interferons. Second, RT-PCR analysis did not detect transcripts for OAS1, a classic interferon target gene product, in either WT or H2KD cells (data not shown). Third, OAS1 as well as OAS2 and OAS3 mRNAs were not detected in any of the three sets of independent microarray experiments (data not shown).

Sequence analyses revealed that about 60% of the up-regulated transcripts (21/37) are classical mammalian NMD substrates (Table 2) since they are encoded by genes that could generate mRNAs with an open reading frame (ORF) terminating more than 55 nt upstream of an exon-exon junction (55-nt rule) (50). For example, visual inspection of available 5′ untranslated regions (UTRs) detected that about one-third of the up-regulated transcripts (13/37) have up to eight AUGs upstream of the physiologic start codon. Accordingly, these transcripts contain at least an out-of-frame upstream open reading frame (uORF) (Fig. 6C) and thus a bona fide PTC. Further, browsing Celera's annotated human genome with gene symbol entries revealed that two of the up-regulated transcripts are encoded by genes in which the authentic termination codon is located in the penultimate exon more than 55 nt upstream of an intron (Fig. 6C, downstream intron). This should result in a classical NMD substrate with an exon-exon junction 55 nt downstream of the authentic termination codon. Finally, comparison of up-regulated transcript sequences with sequences in the recently assembled RUST database containing alternative splice forms with NMD features (38) revealed that one-fifth of our up-regulated transcripts (7/37) are encoded by genes bearing a functional alternative exon that, when either omitted from or spliced into a transcript, generates a PTC at least 55 nt upstream of an exon-exon junction (Fig. 6C, PTC through alternative splicing). A similar search against Celera's annotated human genome identified the BAG1 gene, which encodes an antiapoptotic factor (63) and contains a uORF (Table 2), as a candidate that could also give rise to a PTC-bearing alternatively spliced transcript.

To address the question of whether putative RUST substrates do in fact exist in alternatively spliced PTC isoforms, we decided to analyze the transcriptome of the randomly picked transferrin receptor 2 (TfR2) gene, since TfR2 transcripts are up-regulated when NMD is impaired (Table 2) and alternatively spliced PTC-bearing isoforms are present in the RUST

TABLE 2. Selection of up-regulated transcripts in hUPF2-silenced H2KD cells with their putative NMD-causing features

Gene product description	Gene product symbol	Putative NMD motif	Fold increase
Calcium channel, voltage-dependent, L-type, alpha 1D subunit	CACNA1D	5′ uORF	7.4
Hypothetical protein	FLJ22655	5′ uORF	5.1
Phosphorylase, glycogen, muscle	PYGM	5′ uORF	4.2
Protein tyrosine phosphatase, nonreceptor type 21	PTPN21	5′ uORF	3.5
Tumor necrosis factor receptor superfamily, member 11b	TNFRSF11B	5′ uORF	3.4
Transmembrane 4 superfamily member 12	TM4SF12	5′ uORF	2.8
Homo sapiens calcium channel beta 2a subunit	CACNB2	5′ uORF	2.8
Chromosome 10 open reading frame 28	C10ORF28	5′ uORF	2.5
Neuropilin 1	NRP1	5′ uORF	2.4
Bone morphogenetic protein 5	BMP5	5′ uORF	2.3
BCL2-associated athanogene	BAG1	5′ uORF	2.2
Chromosome 11 open reading frame 8	C11ORF8	5′ uORF	2.2
Transmembrane 4 superfamily member 3	TM4SF3	5′ uORF	2.2
KH domain containing, RNA binding, signal transduction associated 3	KHDRBS3	Downstream intron	4.9
Neogenin homolog 1 (chicken)	NEO1	Downstream intron	4.1
KH domain containing, RNA binding, signal transduction associated 3	KHDRBS3	PTC through alternative splicing	4.9
Sarcosin, sarcomeric muscle protein	KBTBD10	PTC through alternative splicing	2.8
Hypothetical protein	MDS018	PTC through alternative splicing	2.7
Down syndrome critical region gene 1	DSCR1	PTC through alternative splicing	2.4
Transferrin receptor 2	TFR2	PTC through alternative splicing	2.4
Tumor necrosis factor, alpha-induced protein 3	TNFAIP3	PTC through alternative splicing	2.4
Chromosome 11 open reading frame 8	C11ORF8	PTC through alternative splicing	2.2
BCL2-associated athanogene	BAG1	PTC through alternative splicing	2.2

database. TfR2, a type II transmembrane protein, was identified based on its significant homology to TfR1 (27). Like TfR1, it mediates the cellular uptake of transferrin-bound iron, although its affinity to transferrin is lower than that of TfR1. In contrast to TfR1 mRNA levels, levels of TfR2 transcripts are not controlled by cellular iron levels, since they lack an iron responsive element in their 3′ untranslated region.

To investigate the extent of TfR2 PTC isoforms in HeLa cells by RT-PCR, we designed PCR primers to amplify fragments spanning exons 6 to 18, since PTC-containing alternatively or incorrectly spliced TfR2 transcripts lacking exons in this region are described in the Expressed Sequence Tags as well as Celera's annotated human genome database. Besides the expected and correctly spliced 1,436-nt fragment (Fig. 7A, band A), additional smaller bands could be detected by ethidium bromide (EtBr) staining. To reveal their identity, EtBr-stained bands A to F were individually excised from both lanes of the agarose gel, eluted, ligated into a TA cloning vector, and subjected to DNA sequencing. This analysis revealed a surprisingly diverse repertoire of TfR2 nonsense splice isoforms. Only 4 of the 17 different splice variants identified in this study represent a TfR2 isoform without a PTC (A1, B1, C1, and E2; schematically shown in Fig. 7B). Many are alternatively or maybe incorrectly spliced TfR2 isoforms that skipped exons 7 and 8 (B2, C2, D1, D3 to D5, E1, E3, E4, and F1 to F3), thereby generating a PTC in exon 10 (B2, C2, D4, E1, and F2) and, if exon 10 is additionally omitted, in exon 11 (D1, D3, D5, E3, E4, F1, and F3). In addition, exon 12 (F1) and exons 16 and 17 (C1, E2, F2, and F3) can also be alternatively spliced. We also detected nonsense transcripts that either retained the entire intron between exons 12 and 13 (D1) or between exons 15 and 16 (B2, D3, and D5) or retained part of the intron between exons 8 and 9 (D2). Finally, alternative splice acceptor sites in exons 10 (D4), 12 (D5 and E4), and 16 (E1) as well as an alternative splice donor site in exon 10 (E1) were utilized. It should also be mentioned that all of our sequenced transcripts contained exons 13 and 14 with splice acceptor and donor usage sites as predicted by the GenBank entry (accession no. NM_003227), which clearly contradicts the splice acceptor and donor usage sites of these exons listed in Ensembl (gene identification no. ENSG00000106327).

Sequencing of several clones from each ligation also revealed that five of the six bands (B to F) contained more than one TfR2 isoform. Some bands are composed of PTC-bearing as well as sense transcripts (bands B, C, and E), whereas others apparently contain only PTC (bands D and F) or only sense TfR2 isoforms (band A). Therefore, it was surprising that a rough estimate of the EtBr stainings shown in Fig. 7A revealed a more intense signal for band A in hUPF2-silenced H2KD cells. Since we sequenced only some clones from band A of both WT and H2KD cells, it is possible that these bands also contain PTC isoforms that, due to similar sizes, cannot be separated from the correctly spliced sense transcript. For example, band A could contain a PTC isoform that retained intron 15, which would result in a 1,521-bp-long PTC isoform. If such a PTC transcript is present in band A, we would expect that its relative abundance increases in band A from hUPF2-silenced H2KD cells; in contrast, levels of the 1,436-nt sense transcript should not be affected in hUPF2-silenced cells. To address this idea, we isolated band A of WT and H2KD cells from agarose gels, subjected the DNA to PCR with primers annealing to exons 15 and 16, and separated the PCR fragments on an agarose gel (Fig. 7C). As predicted, we detected by PCR two EtBr-stained bands in DNA from band A of both WT and H2KD RT-PCRs; the upper band has the expected length of a fragment with the retained intron between exons 15 and 16 (intron-containing nonsense transcript), and the lower band represents a fragment with correctly spliced exons 15 and 16 (sense transcript). When we compared the EtBr signals of PCRs with purified 1:5 serially diluted band A DNA from WT

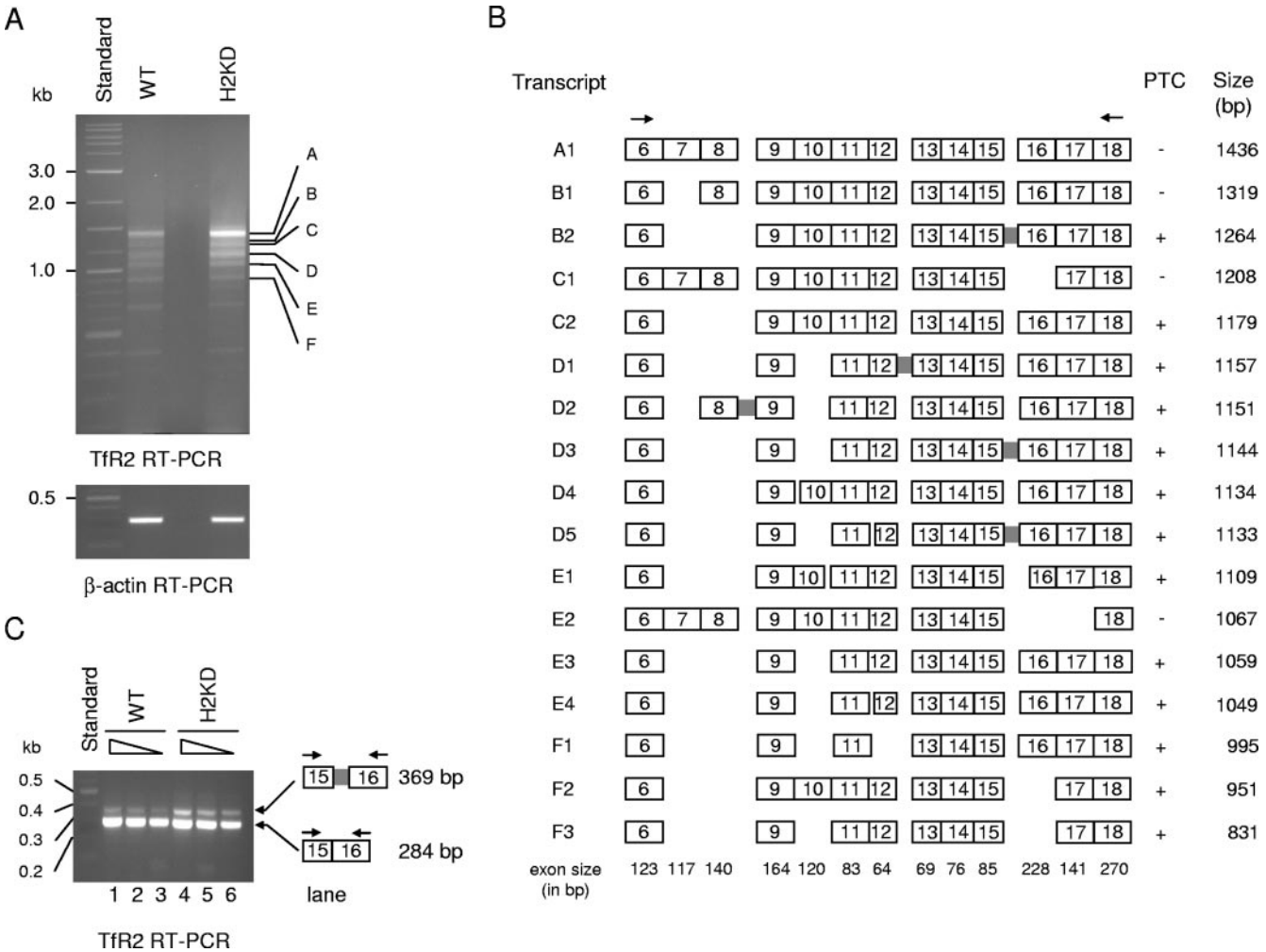

FIG. 7. Analysis of alternatively spliced TfR2 isoforms for the presence of premature termination codons. (A) Total RNA from WT and H2KD cells was subjected to RT-PCR analysis with primers specific for exons 6 and 18 of TfR2. PCR products were separated on a 1.0% agarose gel and detected with ethidium bromide. Size standards of 100 bp and 1 kb are shown on the left. RT-PCR for β-actin served as a control for equal loading of cDNA. (B) Detection of alternative TfR2 splice isoforms by sequence analysis of cloned bands A to F in panel A. RT-PCR products from WT and H2KD cDNAs (bands A to F) from the gel shown in panel A were excised, purified, and cloned. Restriction digest of recombinant plasmids revealed different insert sizes. Several sequences were obtained from each cloned band. An overview of the observed TfR2 splicing patterns is schematically shown. Exon sizes are shown at the bottom, while the presence (+) or absence (−) of a PTC and the size of the PCR product are indicated on the right. Retained introns (the B2, D1, D2, D3, and D5 transcripts) are shown as gray boxes. The D4, D5, E1, and E4 transcripts use alternative splice acceptor sites, while the E1 transcript also uses an alternative splice donor site. Note that exons and introns are not drawn to scale. (C) Detection of alternative TfR2 splice products in band A. Serial dilutions of excised band A from WT and H2KD cells were subjected to PCR analysis with TfR2 primers specific for exons 15 and 16. PCR products were separated on a 1.5% agarose gel and visualized by ethidium bromide staining. A 100-bp size standard is shown on the left, while an overview of the expected TfR2 splicing patterns is schematically shown on the right.

and H2KD cells, we found that the signal of the 284-nt sense transcript is slightly weaker in H2KD cells than that of the corresponding band in WT cells; yet, the signal of the 369-nt intron-containing nonsense transcript is clearly increased in H2KD cells (Fig. 7C, compare lanes 3 and 6) Hence, the relative abundance of a PTC-containing transcript with a retained intron 15 increases in hUPF2-silenced HeLa cells, whereas levels of transcripts lacking a nonsense codon are not affected by hUPF2 silencing. Based on these findings, one could speculate that TfR2 is indeed a RUST substrate and that NMD in cooperation with the regulated retention or removal of an intron controls levels of functional TfR2 mRNA.

In summary, alternative incorrect or incomplete splicing of primary TfR2 transcripts leads to bona fide NMD substrates, which accumulate if the NMD pathway is impaired. These findings could provide another example of a functional gene whose expression is regulated by RUST and therefore by NMD. Whether the retention of introns or the usage of alternative splice sites in TfR2 pre-mRNA is part of a regulatory loop or represents a measure of incomplete or incorrect splicing is not known.

Comparative transcriptome analyses in hUPF2- and hUPF1-silenced HeLa cells. A genome-wide microarray analysis was recently performed by Mendell and coworkers with transiently hUPF1-silenced HeLa cells (47). When we compared the 37 transcripts up-regulated in our stably hUPF2-silenced HeLa cells with the 197 transcripts up-regulated in hUPF1-silenced HeLa cells (47), only 4 transcripts (DSIPI, SLIT2, BAG1, and

DSCR1) were up-regulated more than twofold in both our hUPF2-silenced and in Mendell's hUPF1-silenced HeLa cells (see Table S2 in the supplemental material).

To address the question of whether the 33 remaining transcripts up-regulated in our hUPF2-silenced HeLa cells could at all be detected with the microarray chip used in the study by Mendell et al., we compared signals of genes up-regulated in stably hUPF2-silenced HeLa cells (this study) with signals obtained for corresponding genes in hUPF1-silenced HeLa cells (47). This comparative analysis revealed that nine of the hUPF2-controlled transcripts could not be detected in the study by Mendell et al. since the corresponding DNA oligonucleotide probes were not spotted on the microarray chip. Signals for four transcripts were decreased less than twofold, and one transcript did not change in the microarray analysis by Mendell et al. More interestingly, signals for 19 transcripts up-regulated in our hUPF2-silenced HeLa cells could not be detected in the microarray data set of the study by Mendell et al., although the corresponding oligonucleotide probes were spotted on the microarray chip. Thus, 19 of our 33 hUPF2 regulated transcripts could be putative hUPF2-specific targets.

Inversely, when we compared signals of the 197 genes up-regulated in hUPF1-silenced HeLa cells (47) with signals obtained for corresponding genes in our hUPF2-silenced HeLa cells, we found that oligonucleotides for 22 of the hUPF1-controlled transcripts were not spotted on our microarray chip. Further, signals for 45 transcripts were decreased (but only 3 by more than twofold), and signals for 92 mRNAs were increased (but only 4 by more than twofold) in our microarray data set. Since we considered in our screen only transcripts that increased more than twofold, we identified by comparative analysis of our microarray data set and that from the study by Mendell et al. only four transcripts (SLIT2, BAG-1, DSCR1, and DSIPI) that are susceptible to both hUPF1 and hUPF2 knockdowns. We also identified 38 transcripts that were up-regulated in the Mendell group's microarray data set with RNA from hUPF1-silenced HeLa cells but did not give a signal in our microarray analysis despite the fact that the corresponding DNA oligonucleotides were included on our microarray chip. These results show that most transcripts susceptible to an hUPF1 knockdown are not targeted equally as well as NMD substrates in stably hUPF2-silenced HeLa cells and suggest the possibility of hUPF1- and hUPF2-specific NMD complexes with only a partial target overlap.

Differences in the pattern of NMD targets in hUPF2-silenced (this study) and hUPF1-silenced (47) HeLa cells could however be attributed to the use of different transfection strategies (stable versus transient) and/or to clonal differences of the HeLa line used in the two studies. To exclude these trivial explanations and to confirm that hUPF2-regulated transcripts are not affected by an hUPF1 knockdown, we transiently silenced hUPF1 and hUPF2 along with lamin A/C as a negative control with siRNA in our HeLa cells and quantified the effect of the knockdowns on levels of two hUPF2-regulated transcripts (Fig. 6B, CACNB2 and FLJ22655). We also included in our analysis BAG1, which is up-regulated after hUPF1 (47) and hUPF2 (microarray data from our study) knockdowns, and hSMG-5, which is up-regulated after hUPF1 knockdown (47) but does not change after hUPF2 knockdown in our HeLa cells (microarray data from our study). Western blot analysis of serially diluted cellular lysates 48 h after transfection of siRNA revealed the successful down-regulation of hUPF2, hUPF1, and lamin A/C (Fig. 8A). More importantly, qRT-PCR analysis confirmed our microarray data (see Table S2 in the supplemental material) (Fig. 6B) and that of Mendell et al. (see Table S2 in the supplemental material) (47), i.e., CACNB2 and FLJ22655 levels are affected only by an hUPF2 but not by an hUPF1 knockdown, while signals for the positive control BAG1 increased in both hUPF1- and hUPF2-silenced HeLa cells 4.0- and 2.9-fold, respectively (Fig. 8B). Conversely, hSMG-5, a putative hUPF1-specific target, was affected only by an hUPF1 but not by an hUPF2 knockdown (Fig. 8B).

Although our pool of data is too small to draw solid conclusions at this point, our findings suggest that hUPF1- and hUPF2-specific NMD complexes with only partially overlapping substrate specificities could exist in mammalian cells.

DISCUSSION

The major goal of this study was to determine whether NMD has other functions in addition to removing aberrantly spliced transcripts (22) and viral genomic RNAs converted by RNA editing enzymes into nonsense transcripts (6) as well as aberrant Ig and T-cell receptor mRNA encoded by unproductively rearranged Ig and T-cell receptor genes (4, 26, 39). For example, NMD is required for regulating the levels of mRNAs encoding certain selenoproteins (49) and might be involved in a pathway called RUST (38). RUST combines alternative splicing and NMD as a novel pathway to posttranscriptionally control the expression of genes. Few examples exist for such a coupling in *C. elegans* for transcripts encoding ribosomal proteins (48) and in human cells for the splicing factor SC35 (62) and the polypyrimidine tract binding protein (69). Further evidence for NMD's role in gene expression comes from genome-wide expression profiling of yeast strains bearing single or combinatorial deletions of *UPF1*, *UPF2*, or *UPF3*, which revealed that 4 to 12% of the yeast transcriptome changed in NMD-deficient cells (21, 37).

Genome-wide transcriptome analysis in NMD-impaired human cells. At the beginning of our studies, a genome-wide and systematic analysis of endogenous transcripts regulated by mammalian NMD had not yet been performed. We therefore performed microarray analyses with WT and hUPF2-silenced human HeLa cells and found that about 3.9% of the approximately 2,400 detected transcripts of the Affymetrix HG-U133A chip changed their abundance in hUPF2-silenced HeLa cells (see Table S1 in the supplemental material). The changes in transcript levels in hUPF2-silenced H2KD cells are specific for hUPF2 silencing, since transient RNA interference in HeLa cells employing an hUPF2-specific siRNA with a sequence different from that expressed from the pSUPER vector confirmed the up- and down-regulation of selected transcripts observed in our DNA chip experiments. As expected for a negative control, transfection with lamin A/C siRNA had no effect on selected transcripts that were changed in HeLa cells transiently transfected with hUPF2 siRNA (data not shown). Hence, we conclude that the differences in mRNA abundance observed in our microarray experiments are specific for hUPF2.

We detected 37 up-regulated transcripts but also an almost equal number of down-regulated genes (see Table S1 in the

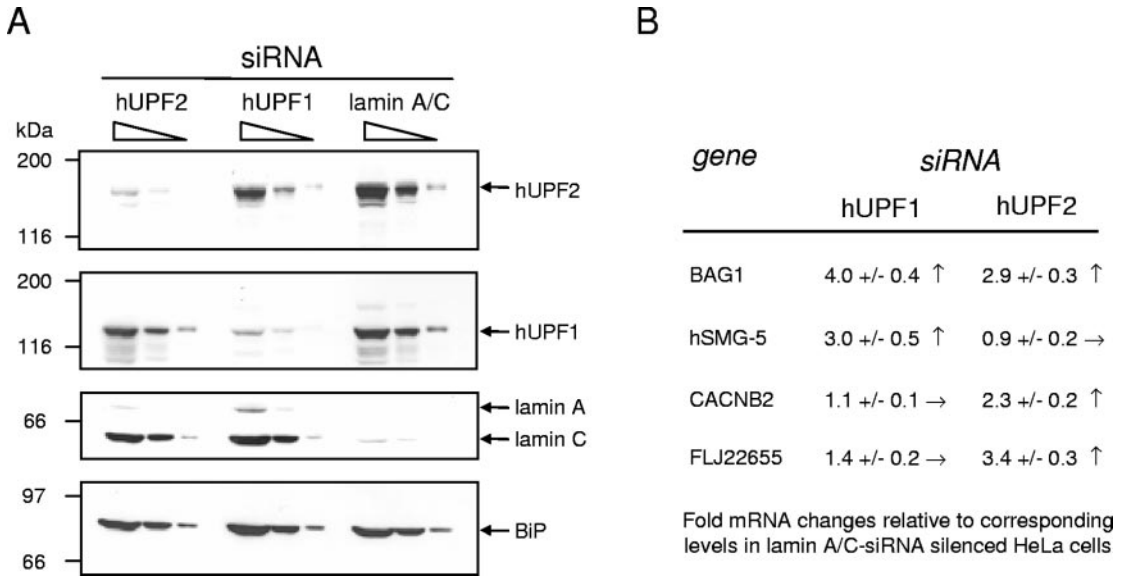

FIG. 8. Comparative qRT-PCR analysis of selected mRNA levels in transiently hUPF1- and hUPF2-silenced HeLa cells. (A) Western blot analysis. Threefold serially diluted cellular lysates starting from 4.5×10^5 HeLa cells transiently transfected with hUPF2 siRNA, hUPF1 siRNA, and lamin A/C siRNA were analyzed as described in the legend to Fig. 4B by stepwise immunoblotting the same membrane with antibodies against hUPF2, hUPF1, and lamin A/C. Equal protein loading was assessed with antibodies against BiP. Molecular masses of standard proteins are indicated in kDa on the left, and the positions of the respective protein bands are indicated on the right of the blots. Results represent one of at least two independent experiments. (B) Quantitative RT-PCR analysis. qRT-PCR values were normalized to β-actin mRNA levels. Relative amounts of respective mRNAs in lamin A/C siRNA-transfected HeLa cells were set to 1, and mRNA changes (*n*-fold) were determined by dividing relative signals of the respective gene in hUPF1- and hUPF2-silenced cells by that in lamin A/C-silenced cells. Average mRNA changes (*n*-fold) and standard deviations of at least four independent qRT-PCR assays (triplicates for each) are shown.

supplemental material). Similar results have been published by Mendell and coworkers for HeLa cells transiently silenced with hUPF1 siRNA (47). Both of these findings are in contrast to expression profiles in NMD-deficient yeast strains, which revealed that more than 95% of the NMD substrates are up-regulated (21, 37). One way to explain the high number of down-regulated transcripts in NMD-silenced mammalian cells is that the expression levels of some mRNAs encoding transcriptional silencers or mRNA destabilizers are controlled by RUST, a mechanism that has been described only for *C. elegans* and mammals but not for yeast (48, 62, 69). In support of this, transcripts for putative RNA binding proteins (KHDRBS3) and factors that directly or indirectly control gene expression (DSCR1, TNFRSF11B, BMP5, and TNFAIP3) are up-regulated in hUPF2-silenced cells, and several transcripts encoding transcription factors were detected in hUPF1-silenced cells (47). Further, NMD-affected transcription factors in yeast have been described previously (28). A selection of down-regulated transcripts in H2KD cells along with their biological roles is shown in Table 3.

Although our up-regulated transcripts do not cluster into a specific biological pathway (see Table S1 in the supplemental material), sequence analysis clearly identified potential NMD features in 21 of the 37 up-regulated transcripts. Fifteen of the NMD targets contain an ORF without a PTC, which classifies them as physiological and functional transcripts. Yet, they carry either several out-of-frame AUGs (13/21) in their 5′ UTR or are encoded from a gene containing an intron down-

TABLE 3. Selection of down-regulated transcripts in hUPF2-silenced H2KD cells with their biological function

Gene product description	Gene product symbol	Biological function(s) (GeneCards database)	Fold decrease
Serine (or cysteine) proteinase inhibitor, clade B (ovalbumin), member 5	SERPINB5	Tumor suppressor	8.7
Cytoplasmic FMR1 interacting protein 1	CYFIP2	p53-inducible protein	6.1
Ankyrin repeat domain 15	ANKRD15	Tumorigenesis of renal cell carcinoma	5.5
Calcium/calmodulin-dependent protein kinase II inhibitor alpha	PRO1489	Probably kinase activity	3.4
Hairy/enhancer-of-split related with YRPW motif 1	HEY1	Transcription factor	3.1
Clusterin	CLU	Associated with programmed cell death (apoptosis)	3.0
UPF2 regulator of nonsense transcripts homolog (yeast)	UPF2	RNA binding, protein biosynthesis	2.3
Transmembrane 4 superfamily member tetraspan	NET-6	Putative signal transduction	2.3

stream of the penultimate exon with the authentic stop codon (2/21), both of which would mark the respective transcript as a genuine NMD substrate. Therefore, these transcripts are new and true physiologic NMD substrates.

We also identified eight genes that encode differentially spliced nonsense transcripts and could therefore be controlled by RUST. As expected for a RUST candidate, we indeed detected multiple differentially spliced nonsense TfR2 transcripts (Fig. 7A and B) and verified the increase in the abundance of one of the nonsense isoforms in H2KD cells (Fig. 7C). However, whether the eight transcripts are true RUST substrates requires further investigation.

Differences in hUPF1 und hUPF2 substrate specificity. Although about half of the up-regulated transcripts identified in hUPF2-silenced as well as in hUPF1-silenced HeLa cells (47) match one of three classes of NMD substrates (Table 2), there are three important differences between our study and that of Mendell and coworkers. First, only 4 (DSIPI, SLIT2, BAG1, and DSCR1) of our 37 up-regulated transcripts were also up-regulated in hUPF1-silenced HeLa cells, 2 of which (BAG1 and DSCR1) carry known NMD features (Table 2); second, about 2.5 times more potential NMD targets were identified in the screen by Mendell et al. (9.3% compared to 3.9%). And third, comparison of transcripts up-regulated in our hUPF2-silenced HeLa cells to those in the microarray data set of Mendell et al. (see Table S2 in the supplemental material) (47) and comparison of transcripts up-regulated in hUPF1-silenced HeLa cells of Mendell et al. to those in our microarray data set (see Table S2 in the supplemental material) identified 19 transcripts that were up-regulated at least twofold in only our hUPF2-silenced HeLa cells and 38 transcripts up-regulated in only hUPF1-silenced HeLa cells of Mendell et al. (47).

Therefore, it seems as if the majority of transcripts up-regulated under our conditions in stable hUPF2-silenced HeLa cells are regulated only by hUPF2 but not by hUPF1, suggesting the existence of hUPF1- and hUPF2-specific NMD complexes with minimal overlapping substrate specificity.

Support for this hypothesis comes first from our finding that levels of two of our hUPF2-regulated transcripts (Fig. 6B, CACNB2 and FLJ22655) are affected only by an hUPF2 knockdown and not by an hUPF1 knockdown (Fig. 8B). Since we used the same HeLa line for these experiments, we can exclude experimental variations and clonal differences.

The lower numbers of hUPF2 targets might be due to the fact that we used more stringent parameters. For example, changing the *P* values from 0.001 in our study to, e.g., 0.05 would in fact lead to an increase in differently expressed messages. The numbers of regulated transcripts in our study, however, would still be well below the numbers observed in hUPF1-silenced HeLa cells. In addition, while Mendell et al. used a cutoff of 1.9-fold and repeated their microarrays only twice, we considered as putative hUPF2 targets only mRNAs that were at least 2-fold regulated in three independent microarray experiments. Further, Mendell et al. used a different microarray chip. Due to the dynamic nature of public databases, probe sets for these sequences will not be identical and in some cases will be represented by a completely new probe set. As a result, data generated with different versions of human arrays may not produce concordant results. Lastly, these analyses were done in different laboratories, which might account for some of the differences observed between our study and that of Mendell and coworkers.

Effect of hUPF2 silencing on cell growth. The second interesting and surprising finding of our study is that stably hUPF2-silenced HeLa clones could easily be established and cultured for several months without gross differences in survival and growth rate (Fig. 6). Therefore, hUPF2 does not seem to be essential for growth of tumor lines. However, residual amounts of hUPF2 could be sufficient for viability, and perhaps a complete hUPF2 knockout would have a more severe phenotype. On the one hand, this was not surprising since the deletion of any of the hUPF orthologs in yeast and *C. elegans* had only a minor effect on overall growth and development (1, 23). In contrast, homozygous deletion of mUPF1/rent1 in the mouse genome leads to an embryonic lethal phenotype at a very early stage and to apoptosis of cultured mUPF1/rent1$^{-/-}$ blastocysts (44). Similarly, stable hUPF1-deficient lines by either shRNA-mediated silencing in HeLa cells or inactivation of hUPF1 through a classical homologous recombination in the chicken line DT40 could not be established (J. Wittmann, M. Selg, D. Fuchs, and H.-M. Jäck, unpublished data). Therefore, hUPF1 might have functions different from those of hUPF2. For example, yeast Upf1p is involved in translational termination (67), and hUPF1 is required for skipping of PTC-containing exons in human cells (46). Further, hUPF1 could modulate replication/transcription processes since it copurifies with DNA polymerase delta (10). Finally, hUPF1 could play additional roles in splicing, intracellular transport, polarization, and stabilization of certain mRNAs. In support of this idea, Staufen1, a protein involved in RNA localization, has been identified as an hUPF1 interaction partner and recruits hUPF1 to the 3′ UTRs of certain mRNAs, which then elicits mRNA decay (30). In addition, a yeast two-hybrid screen with hUPF1 identified p32 (J. Strande, M. Selg, and H.-M. Jäck, unpublished data), a factor tightly associated with the splicing factor ASF/SF2 (31).

Effect of hUPF2 silencing on hUPF1 phosphorylation. The third interesting and novel finding is that hUPF2 silencing negatively affects the phosphorylation of hUPF1 (Fig. 4). Phosphorylation of the RNA helicase hUPF1 as well as its *C. elegans* ortholog SMG-2 is controlled by the cooperative action of the Ser/Thr kinase hSMG-1 and a phosphatase complex consisting of hSMG-5 and -7 and the protein phosphatase 2A (2, 51). hUPF2 could regulate phosphorylation of hUPF1 by either directly controlling the hSMG-1 kinase, stabilizing phosphorylated hUPF1, or preventing the association of hUPF1 with the phosphatase complex. Indeed, tandem affinity purification and gel filtration studies identified two hUPF1-containing multimeric complexes: one consists of hUPF1, hUPF2, and the long isoform of hUPF3a, whereas the other lacks hUPF2 and the long isoform of hUPF3a but contains hUPF1 and the short isoform of hUPF3a (51, 57). Therefore, hUPF2 might reduce nonsense mRNA levels indirectly by modulating hUPF1 activity via phosphorylation rather than acting directly on nonsense mRNA. Since some hUPF1 is still phosphorylated in hUPF2-silenced HeLa cells, hUPF1 should be enzymatically active. However, hypophosphorylation could have changed hUPF1's activity and substrate specificity, which could explain the qualitative and quantitative differences observed between expression profiles of hUPF2-silenced (this study) and hUPF1-

silenced (47) HeLa cells. hUPF2 very likely does not control phosphorylation of hUPF1 by affecting expression of hSMG-5 and hSMG-6 since, in contrast to hUPF1 silencing (47), a stable hUPF2 knockdown by RNAi has no effect on hSMG-5 and hSMG-6 mRNA levels (data not shown). In summary, we showed that hUPF2 directly or indirectly controls phosphorylation of hUPF1 and provided first evidence that hUPF1- and hUPF2-specific NMD complexes with overlapping and different substrate profiles might exist. Based on our findings and those of Mendell et al. (47), we suggest that NMD is important not only for removing aberrant mRNA but also for posttranscriptional regulation of a selected pool of genes.

ACKNOWLEDGMENTS

Part of this work was supported by the Human Frontier Science Program, the Deutsche Forschungsgemeinschaft (DFG), and the Hertha Löw Foundation to H.-M. Jäck.

We thank Reuven Agami for providing pSUPER; Andreas Kulozik for β-globin WT and nonsense (PTC) constructs; Joachim Lingner and Claus Azzalin for pSUPER-E8 and -E10; Ludger Klein-Hitpass for performing DNA microarray experiments; Brett Lane for help in preparing hUPF2 antibodies; Anja Haude and Edith Roth for technical assistance; and Harald Bradl, Dirk Mielenz, Johannes Lutz, and Christian Vettermann for comments on the manuscript.

REFERENCES

1. **Altamura, N., O. Groudinsky, G. Dujardin, and P. P. Slonimski.** 1992. *NAM7* nuclear gene encodes a novel member of a family of helicases with a Zn-ligand motif and is involved in mitochondrial functions in *Saccharomyces cerevisiae*. J. Mol. Biol. **224:**575–587.
2. **Anders, K. R., A. Grimson, and P. Anderson.** 2003. SMG-5, required for *C. elegans* nonsense-mediated mRNA decay, associates with SMG-2 and protein phosphatase 2A. EMBO J. **22:**641–650.
3. **Applequist, S. E., M. Selg, C. Raman, and H. M. Jäck.** 1997. Cloning and characterization of HUPF1, a human homolog of the Saccharomyces cerevisiae nonsense mRNA-reducing UPF1 protein. Nucleic Acids Res. **25:**814–821.
4. **Baumann, B., M. J. Potash, and G. Kohler.** 1985. Consequences of frameshift mutations at the immunoglobulin heavy chain locus of the mouse. EMBO J. **4:**351–359.
5. **Bhattacharya, A., K. Czaplinski, P. Trifillis, F. He, A. Jacobson, and S. W. Peltz.** 2000. Characterization of the biochemical properties of the human Upf1 gene product that is involved in nonsense-mediated mRNA decay. RNA **6:**1226–1235.
6. **Bishop, K. N., R. K. Holmes, A. M. Sheehy, and M. H. Malim.** 2004. APOBEC-mediated editing of viral RNA. Science **305:**645.
7. **Bradl, H., J. Wittmann, D. Milius, C. Vettermann, and H. M. Jäck.** 2003. Interaction of murine precursor B cell receptor with stroma cells is controlled by the unique tail of lambda 5 and stroma cell-associated heparan sulfate. J. Immunol. **171:**2338–2348.
8. **Bridge, A. J., S. Pebernard, A. Ducraux, A. L. Nicoulaz, and R. Iggo.** 2003. Induction of an interferon response by RNAi vectors in mammalian cells. Nat. Genet. **34:**263–264.
9. **Brummelkamp, T. R., R. Bernards, and R. Agami.** 2002. A system for stable expression of short interfering RNAs in mammalian cells. Science **296:**550–553.
10. **Carastro, L. M., C. K. Tan, M. Selg, H. M. Jäck, A. G. So, and K. M. Downey.** 2002. Identification of delta helicase as the bovine homolog of HUPF1: demonstration of an interaction with the third subunit of DNA polymerase delta. Nucleic Acids Res. **30:**2232–2243.
11. **Chiu, S. Y., G. Serin, O. Ohara, and L. E. Maquat.** 2003. Characterization of human Smg5/7a: a protein with similarities to *Caenorhabditis elegans* SMG5 and SMG7 that functions in the dephosphorylation of Upf1. RNA **9:**77–87.
12. **Clemens, M. J., and A. Elia.** 1997. The double-stranded RNA-dependent protein kinase PKR: structure and function. J. Interferon Cytokine Res. **17:**503–524.
13. **Culbertson, M. R., and P. F. Leeds.** 2003. Looking at mRNA decay pathways through the window of molecular evolution. Curr. Opin. Genet. Dev. **13:**207–214.
14. **Denning, G., L. Jamieson, L. E. Maquat, E. A. Thompson, and A. P. Fields.** 2001. Cloning of a novel phosphatidylinositol kinase-related kinase: characterization of the human SMG-1 RNA surveillance protein. J. Biol. Chem. **25:**22709–22714.
15. **Doench, J. G., C. P. Petersen, and P. A. Sharp.** 2003. siRNAs can function as miRNAs. Genes Dev. **17:**438–442.
16. **Dostie, J., and G. Dreyfuss.** 2002. Translation is required to remove Y14 from mRNAs in the cytoplasm. Curr. Biol. **12:**1060–1067.
17. **Elbashir, S. M., J. Harborth, W. Lendeckel, A. Yalcin, K. Weber, and T. Tuschl.** 2001. Duplexes of 21-nucleotide RNAs mediate RNA interference in cultured mammalian cells. Nature **411:**494–498.
18. **Gatfield, D., L. Unterholzner, F. D. Ciccarelli, P. Bork, and E. Izaurralde.** 2003. Nonsense-mediated mRNA decay in Drosophila: at the intersection of the yeast and mammalian pathways. EMBO J. **22:**3960–3970.
19. **Gossen, M., and H. Bujard.** 1992. Tight control of gene expression in mammalian cells by tetracycline-responsive promoters. Proc. Natl. Acad. Sci. USA **89:**5547–5551.
20. **Grimson, A., S. O'Connor, C. L. Newman, and P. Anderson.** 2004. SMG-1 is a phosphatidylinositol kinase-related protein kinase required for nonsense-mediated mRNA decay in *Caenorhabditis elegans*. Mol. Cell. Biol. **24:**7483–7490.
21. **He, F., X. Li, P. Spatrick, R. Casillo, S. Dong, and A. Jacobson.** 2003. Genome-wide analysis of mRNAs regulated by the nonsense-mediated and 5′ to 3′ mRNA decay pathways in yeast. Mol. Cell **12:**1439–1452.
22. **Hillman, R. T., R. E. Green, and S. E. Brenner.** 2004. An unappreciated role for RNA surveillance. Genome Biol. **2:**R8.
23. **Hodgkin, J., A. Papp, R. Pulak, V. Ambros, and P. Anderson.** 1989. A new kind of informational suppression in the nematode Caenorhabditis elegans. Genetics **123:**301–313.
24. **Ishigaki, Y., X. Li, G. Serin, and L. E. Maquat.** 2001. Evidence for a pioneer round of mRNA translation: mRNAs subject to nonsense-mediated decay in mammalian cells are bound by CBP80 and CBP20. Cell **106:**607–617.
25. **Jäck, H. M., and M. Wabl.** 1988. Immunoglobulin mRNA stability varies during B lymphocyte differentiation. EMBO J. **7:**1041–1046.
26. **Jäck, H. M., J. Berg, and M. Wabl.** 1989. Translation affects immunoglobulin mRNA stability. Eur. J. Immunol. **19:**843–847.
27. **Kawabata, H., R. Yang, T. Hirama, P. T. Vuong, S. Kawano, A. F. Gombart, and H. P. Koeffler.** 1999. Molecular cloning of transferrin receptor 2. A new member of the transferrin receptor-like family. J. Biol. Chem. **274:**20826–20832.
28. **Kebaara, B., T. Nazarenus, R. Taylor, A. Forch, and A. L. Atkin.** 2003. The Upf-dependent decay of wild-type PPR1 mRNA depends on its 5′-UTR and first 92 ORF nucleotides. Nucleic Acids Res. **31:**3157–3165.
29. **Kim, V. N., N. Kataoka, and G. Dreyfuss.** 2001. Role of the nonsense-mediated decay factor hUpf3 in the splicing-dependent exon-exon junction complex. Science **293:**1832–1836.
30. **Kim, Y. K., L. Furic, L. Desgroseillers, and L. E. Maquat.** 2005. Mammalian Staufen1 recruits Upf1 to specific mRNA 3′UTRs so as to elicit mRNA decay. Cell **120:**195–208.
31. **Krainer, A. R., A. Mayeda, D. Kozak, and G. Binns.** 1991. Functional expression of cloned human splicing factor SF2: homology to RNA-binding proteins, U1 70K and *Drosophila* splicing regulators. Cell **66:**383–394.
32. **Lamba, J. K., M. Adachi, D. Sun, J. Tammur, E. G. Schuetz, R. Allikmets, and J. D. Schuetz.** 2003. Nonsense mediated decay downregulates conserved alternatively spliced ABCC4 transcripts bearing nonsense codons. Hum. Mol. Genet. **12:**99–109.
33. **Leeds, P., J. M. Wood, B.-S. Lee, and M. R. Culbertson.** 1992. Gene products that promote mRNA turnover in *Saccharomyces cerevisiae*. Mol. Cell. Biol. **12:**2165–2177.
34. **Le Hir, H., E. Izaurralde, L. E. Maquat, and M. J. Moore.** 2000. The spliceosome deposits multiple proteins 20–24 nucleotides upstream of mRNA exon-exon junctions. EMBO J. **19:**6860–6869.
35. **Le Hir, H., M. J. Moore, and L. E. Maquat.** 2000. Pre-mRNA splicing alters mRNP composition: evidence for stable association of proteins at exon-exon junctions. Genes Dev. **14:**1098–1108.
36. **Lejeune, F., Y. Ishigaki, X. Li, and L. E. Maquat.** 2002. The exon junction complex is detected on CBP80-bound but not eIF4E-bound mRNA in mammalian cells: dynamics of mRNP remodeling. EMBO J. **21:**3536–3545.
37. **Lelivelt, M. J., and M. R. Culbertson.** 1999. Yeast Upf proteins required for RNA surveillance affect global expression of the yeast transcriptome. Mol. Cell. Biol. **19:**6710–6719.
38. **Lewis, B. P., R. E. Green, and S. E. Brenner.** 2003. Evidence for the widespread coupling of alternative splicing and nonsense-mediated mRNA decay in humans. Proc. Natl. Acad. Sci. USA **100:**189–192.
39. **Li, S., and M. F. Wilkinson.** 1998. Nonsense surveillance in lymphocytes? Immunity **8:**135–141.
40. **Losson, R., and F. Lacroute.** 1979. Interference of nonsense mutations with eukaryotic messenger RNA stability. Proc. Natl. Acad. Sci. USA **76:**5134–5137.
41. **Lykke-Andersen, J., M. D. Shu, and J. A. Steitz.** 2000. Human Upf proteins target an mRNA for nonsense-mediated decay when bound downstream of a termination codon. Cell **103:**1121–1131.
42. **Maquat, L. E.** 1995. When cells stop making sense: effects of nonsense codons on RNA metabolism in vertebrate cells. RNA **1:**453–465.
43. **Maquat, L. E.** 2004. Nonsense-mediated mRNA decay: splicing, translation and mRNP dynamics. Nat. Rev. Mol. Cell Biol. **5:**89–99.
44. **Medghalchi, S. M., P. A. Frischmeyer, J. T. Mendell, A. G. Kelly, A. M. Lawler, and H. C. Dietz.** 2001. Rent1, a trans-effector of nonsense-mediated

mRNA decay, is essential for mammalian embryonic viability. Hum. Mol. Genet. **10:**99–105.
45. **Mendell, J. T., S. M. Medghalchi, R. G. Lake, E. N. Noensie, and H. C. Dietz.** 2000. Novel Upf2p orthologues suggest a functional link between translation initiation and nonsense surveillance complexes. Mol. Cell. Biol. **20:**8944–8957.
46. **Mendell, J. T., C. M. ap Rhys, and H. C. Dietz.** 2002. Separable roles for rent1/hUpf1 in altered splicing and decay of nonsense transcripts. Science **298:**419–422.
47. **Mendell, J. T., N. A. Sharifi, J. L. Meyers, F. Martinez-Murillo, and H. C. Dietz.** 2004. Nonsense surveillance regulates expression of diverse classes of mammalian transcripts and mutes genomic noise. Nat. Genet. **36:**1073–1078.
48. **Mitrovich, Q. M., and P. Anderson.** 2000. Unproductively spliced ribosomal protein mRNAs are natural targets of mRNA surveillance in *C. elegans*. Genes Dev. **14:**2173–2184.
49. **Moriarty, P. M., C. C. Reddy, and L. E. Maquat.** 1998. Selenium deficiency reduces the abundance of mRNA for Se-dependent glutathione peroxidase 1 by a UGA-dependent mechanism likely to be nonsense codon-mediated decay of cytoplasmic mRNA. Mol. Cell. Biol. **18:**2932–2939.
50. **Nagy, E., and L. E. Maquat.** 1998. A rule for termination-codon position within intron-containing genes: when nonsense affects RNA abundance. Trends Biochem. Sci. **23:**198–199.
51. **Ohnishi, T., A. Yamashita, I. Kashima, T. Schell, K. R. Anders, A. Grimson, T. Hachiya, M. W. Hentze, P. Anderson, and S. Ohno.** 2003. Phosphorylation of hUPF1 induces formation of mRNA surveillance complexes containing hSMG-5 and hSMG-7. Mol. Cell **12:**1187–1200.
52. **Orkin, S. H., and S. C. Goff.** 1981. Nonsense and frameshift mutations in β^0-thalassemia detected in cloned β-globin genes. J. Biol. Chem. **256:**9782–9784.
53. **Page, M. F., B. Carr, K. R. Anders, A. Grimson, and P. Anderson.** 1999. SMG-2 is a phosphorylated protein required for mRNA surveillance in *Caenorhabditis elegans* and related to Upf1p of yeast. Mol. Cell. Biol. **19:**5943–5951.
54. **Paillusson, A., N. Hirschi, C. Vallan, C. M. Azzalin, and O. Muhlemann.** 2005. A GFP-based reporter system to monitor nonsense-mediated mRNA decay. Nucleic Acids Res. **33:**e54.
55. **Pal, M., Y. Ishigaki, E. Nagy, and L. E. Maquat.** 2001. Evidence that phosphorylation of human Upf1 protein varies with intracellular location and is mediated by a wortmannin-sensitive and rapamycin-sensitive PI 3-kinase-related kinase signaling pathway. RNA **7:**5–15.
56. **Perlick, H. A., S. M. Medghalchi, F. A. Spencer, R. J. Kendzior, Jr., and H. C. Dietz.** 1996. Mammalian orthologues of a yeast regulator of nonsense transcript stability. Proc. Natl. Acad. Sci. USA **93:**10928–10932.
57. **Schell, T., T. Kocher, M. Wilm, B. Seraphin, A. E. Kulozik, and M. W. Hentze.** 2003. Complexes between the nonsense-mediated mRNA decay pathway factor human upf1 (up-frameshift protein 1) and essential nonsense-mediated mRNA decay factors in HeLa cells. Biochem. J. **373:**775–783.
58. **Serin, G., A. Gersappe, J. D. Black, R. Aronoff, and L. E. Maquat.** 2001. Identification and characterization of human orthologues to *Saccharomyces cerevisiae* Upf2 protein and Upf3 protein (*Caenorhabditis elegans* SMG-4). Mol. Cell. Biol. **21:**209–223.
59. **Shiloh, Y.** 2003. ATM and related protein kinases: safeguarding genome integrity. Nat. Rev. Cancer **3:**155–168.
60. **Sledz, C. A., M. Holko, M. J. de Veer, R. H. Silverman, and B. R. Williams.** 2003. Activation of the interferon system by short-interfering RNAs. Nat. Cell Biol. **5:**834–839.
61. **Sun, X., H. A. Perlick, H. C. Dietz, and L. E. Maquat.** 1998. A mutated human homologue to yeast Upf1 protein has a dominant-negative effect on the decay of nonsense-containing mRNAs in mammalian cells. Proc. Natl. Acad. Sci. USA **95:**10009–10014.
62. **Sureau, A., R. Gattoni, Y. Dooghe, J. Stevenin, and J. Soret.** 2001. SC35 autoregulates its expression by promoting splicing events that destabilize its mRNAs. EMBO J. **20:**1785–1796.
63. **Takayama, S., T. Sato, S. Krajewski, K. Kochel, S. Irie, J. A. Millan, and J. C. Reed.** 1995. Cloning and functional analysis of BAG-1: a novel Bcl-2-binding protein with anti-cell death activity. Cell **80:**279–284.
64. **Thermann, R., G. Neu-Yilik, A. Deters, U. Frede, K. Wehr, C. Hagemeier, M. W. Hentze, and A. E. Kulozik.** 1998. Binary specification of nonsense codons by splicing and cytoplasmic translation. EMBO J. **17:**3484–3494.
65. **van Leeuwen, F. W., D. P. de Kleijn, H. H. van den Hurk, A. Neubauer, M. A. Sonnemans, J.-A. Sluijs, S. Koycu, R. D. Ramdjielal, A. Salehi, G. J. Martens, F. G. Grosveld, J. Peter, H. Burbach, and E. M. Hol.** 1998. Frameshift mutants of beta amyloid precursor protein and ubiquitin-B in Alzheimer's and Down patients. Science **279:**242–247.
66. **Wang, J., V. M. Vock, S. Li, O. R. Olivas, M. F. Wilkinson.** 2002. A quality control pathway that down-regulates aberrant T-cell receptor (TCR) transcripts by a mechanism requiring UPF2 and translation. J. Biol. Chem. **277:**18489–18493.
67. **Weng, Y., K. Czaplinski, and S. W. Peltz.** 1996. Identification and characterization of mutations in the *UPF1* gene that affect nonsense suppression and the formation of the Upf protein complex but not mRNA turnover. Mol. Cell. Biol. **16:**5491–5506.
68. **Wilson, G. M., Y. Sun, J. Sellers, H. Lu, N. Penkar, G. Dillard, and G. Brewer.** 1999. Regulation of AUF1 expression via conserved alternatively spliced elements in the 3′ untranslated region. Mol. Cell. Biol. **19:**4056–4064.
69. **Wollerton, M. C., C. Gooding, E. J. Wagner, M. A. Garcia-Blanco, and C. W. Smith.** 2004. Autoregulation of polypyrimidine tract binding protein by alternative splicing leading to nonsense-mediated decay. Mol. Cell **13:**91–100.
70. **Yamashita, A., T. Ohnishi, I. Kashima, Y. Taya, and S. Ohno.** 2001. Human SMG-1, a novel phosphatidylinositol 3-kinase-related protein kinase, associates with components of the mRNA surveillance complex and is involved in the regulation of nonsense-mediated mRNA decay. Genes Dev. **15:**2215–2228.